On the Design of Dual Energy Harvesting Communication Links With Retransmission

Mohit K. Sharma and Chandra R. Murthy, *Senior Member, IEEE*

***Abstract*— In this paper, we consider *retransmission-based* point-to-point *dual* energy harvesting (EH) links, where both the transmitter and receiver are EH nodes (EHNs). The transmitter needs to periodically send a packet to the receiver and the packet is *dropped* if it is not delivered within a given number of slots. The goal is to find a *retransmission index-based* power management policy (RIP), which minimizes the packet drop probability (PDP). To this end, first, we establish the near-optimality of policies that operate in the *energy unconstrained regime (EUR)*, i.e., the regime where the average rate of energy use at each EHN is less than the average harvesting rate. Specifically, we analytically show that for such policies, the gap between the PDP of the dual EH systems with finite and infinite capacity batteries decreases exponentially with the size of the battery at the transmitter and receiver. Next, we show that, in the EUR, the non-convex problem of designing optimal RIPs can be reformulated as a *geometric program*, which leads to a provably convergent and computationally efficient solution. We design the RIPs for both slow and fast fading channels, and with two different retransmission protocols, namely, the automatic repeat request (ARQ) and hybrid ARQ with chase combining. Numerical results obtained through Monte Carlo simulations show that the proposed RIPs outperform the state-of-the-art policies.**

***Index Terms*— Energy harvesting, ARQ, HARQ-CC, packet drop probability, geometric programming, battery size, receiver.**

I. Introduction

AN ENERGY harvesting node (EHN) harvests energy from the environment, e.g., from a solar, wind, piezo-electric, or radio frequency source [1]–[3]. This can improve the lifetime of wireless sensor networks (WSN) which are used in many control and monitoring applications. Dual energy harvesting (EH) links, i.e., point-to-point communication links whose both transmitter and receiver are EHNs [4], are the basic building blocks of EH based WSNs [5]. Dual EH links generalize *mono* EH links [6]–[9], where only one node harvests energy. This generalization makes the design more challenging, as one needs to account for the sporadic energy availability at both the transmitter and receiver, as well as the lack of availability of the energy state of each node at the other node. Also, the spatio-temporal correlation in the energy arrivals at the EHNs needs to be leveraged for obtaining the best possible performance. Due to this, policies designed for mono EH links could in general be sub-optimal for dual EH links (see Fig. 4b). Therefore, the design of reliable dual EH links is an important first step in the design of EH WSNs [10].

The retransmission protocols in conjunction with transmit power control are a good choice for reliable EH links, as they help to mitigate the randomness of the wireless channel as well as of the time-varying EH process [11]–[17]. Retransmission protocols are also part of low power communication standards such as IEEE 802.15.4 [18]. The reliability of retransmission based links with fixed size packets is quantified by the packet drop probability (PDP) [14], [19].

In this work, we consider a dual EH link where a transmitting EHN periodically obtains a measurement, at the beginning of a *frame*. The measurement needs to be delivered to another EHN by the end of the frame; otherwise it is dropped. Each packet can be attempted repeatedly till the end of the frame, provided both nodes have sufficient energy to communicate. Transmission is stopped after successful delivery, and both EHNs save the harvested energy in a finite sized battery for the rest of the frame. The PDP is defined as the average fraction of packets dropped out of all the packets attempted. This model is applicable in scenarios where periodic measurements are taken, and are useful only if they are delivered by a deadline.

The goal of this paper is to design power management policies for dual EH links with retransmission. First, we characterize the impact of the size of the battery at the transmitter and receiver on the PDP performance, for policies that operate in the so-called energy unconstrained regime (EUR). A larger battery size helps the EHNs overcome the randomness in the harvested energy and wireless channel, but it is not clear how large the battery needs to be, in order to obtain near-optimal performance. Next, we design optimal *retransmission index-based policies* (RIPs) to minimize the PDP. An RIP provides an attempt-based prescription for the management of power at the transmitter and receiver, namely, the number of attempts to make and the corresponding power levels. The time-varying and random nature of the harvesting and channel fading processes, as well as the finiteness of the battery capacities, makes the design of optimal RIPs challenging. For example, it is not clear whether a single transmission attempt at a high transmit power will result in better PDP compared to making successive attempts at progressively higher power levels, initializing from a low-power attempt. The answer, in

Manuscript received October 12, 2016; revised February 15, 2017 and March 22, 2017; accepted March 23, 2017. Date of publication April 12, 2017; date of current version June 8, 2017. This work was supported by a research grant from the Aerospace Network Research Consortium. The associate editor coordinating the review of this paper and approving it for publication was C.-H. Lee. *(Corresponding author: Chandra R. Murthy.)*

The authors are with the Department of Electrical and Communication Engineering, Indian Institute of Science, Bangalore 560 012, India (e-mail: mohit@ece.iisc.ernet.in; cmurthy@ece.iisc.ernet.in).

Color versions of one or more of the figures in this paper are available online at http://ieeexplore.ieee.org.

Digital Object Identifier 10.1109/TWC.2017.2691777

turn, depends on the channel coherence time, EH statistics, and the data processing performed at the receiver.

We present the design of RIPs for two different retransmission protocols: *automatic-repeat-request* (ARQ) and hybrid ARQ with chase combining (HARQ-CC). In contrast to ARQ, the receiver in HARQ-CC applies maximal ratio combining to decode a packet using the copies of the packet received in previous attempts. With ARQ, the received signal-to-noise ratio (SNR) in the current attempt determines the probability of packet success; while with HARQ-CC, it depends on the accumulated SNR across all attempts. Due to this, the structure of the optimal RIPs in the two cases are fundamentally different. In addition, we design the RIPs for ARQ and HARQ-CC under both slow and fast fading channels.

A. Related Work

The design of power control policies for mono EH links, where only the transmitter is an EHN, herein referred to as *mono-T* links, has been studied to optimize the delay [7], transmission time [8], throughput [9], and PDP [13]–[15]. Throughput maximizing policies when only the receiver is energy harvesting are designed in [20]. The interested reader is referred to [6] for a review of recent advances in the area of energy harvesting wireless communications.

Arafa and Ulukus [4] present an offline throughput maximizing policy for a dual EH link with an AWGN channel and infinite energy buffers. However, the work in [4] does not consider retransmissions and the time-varying fading channel. Dual EH links with finite sized batteries and ARQ are considered in [11], [12], [16], and [17]. Yadav *et al.* [12] propose to selectively sample the packet, while [11], [16], [17] consider the conventional ARQ, where the entire packet is sampled and decoded, depending on the energy available at the receiver. In [16] and [17], closed-form expressions for the PDP of dual EH links with ARQ and HARQ-CC protocols are obtained. However, [16], [17] do not provide the design of power control policies. Zhou *et al.* [11] propose throughput maximizing policies for fast fading channels, which is obtained using a global search over the space of affine policies. However, the restriction of the search to affine policies may be suboptimal in general. Also, the computational complexity of global search methods is prohibitively large, even for moderate sized batteries. Hence, it is desirable to come up with design procedures whose complexity does not grow with the battery size.

Another important aspect in the design of power policies for EH systems is availability of the battery's state-of-charge (SoC). A majority of the existing literature assumes the availability of perfect SoC information. However, the estimation of SoC could be energy-expensive [21], [22]. Michelusi *et al.* [23] show that the knowledge of the EH statistics can partially compensate for the lack of SoC information. Testa and Zorzi [24] and Srivastava and Koksal [25], present policies that achieve near-optimal utility with 1-bit SoC. On a related note, [11], [14], [15] consider policies for which the transmit power is SoC-independent, e.g., affine policies [11]. However, a systematic procedure for designing SoC-independent policies is not available even for mono EH links. In this paper, we design near-optimal, SoC-independent RIPs, and benchmark them against the state-of-the-art policies. Also, the design of power control policies for HARQ-CC based links has not been considered in the literature. Next, we summarize the main contributions of this work.

B. Contributions

1) We derive both upper and lower bounds on the PDP of dual EH links with finite capacity batteries. The bounds are obtained in terms of the PDP achieved with ideal (infinite capacity) batteries. We analyze the gap between the upper and lower bounds, and show that for policies operating in the EUR, the gap goes to zero exponentially fast with the battery size at the transmitter and receiver. This result not only shows that the bounds are asymptotically tight, it also explicitly characterizes the dependence of the PDP on the size of the batteries (Secs. III and IV).
2) We present a systematic procedure to design near-optimal RIPs for dual EH links with retransmission. The problem formulation is a non-convex mixed integer program, which is known to be strongly NP hard. We solve it in a computationally efficient and provably convergent manner using techniques from geometric programming (GP) (Secs. V and VI-A).
3) The impact of channel coherence time and receiver processing is accounted for by designing the policies for two different retransmission protocols: ARQ and HARQ-CC, as well as for two different modes of channel variation: slow and fast fading channels (Sec. VI).
4) We show that our proposed design procedure can be extended to handle spatially and temporally correlated EH processes (Sec. VII).

These results are useful to determine the order of battery size required for obtaining a desired performance level. In fact, the dependence of the PDP on the battery size is not well understood in the literature, even for mono EH links. Since mono EH links are a special case of dual EH links, our proposed approach can be used to design near-optimal RIPs for this case also. For dual EH links with sufficiently large sized batteries, we show that it is near-optimal to design the power control policies under an average power constraint. Due to this, the complexity of finding the RIP is independent of the size of the batteries. We empirically show that the designed RIPs even outperform the SoC-dependent state-of-the-art policies (see Fig. 7).

II. System Model

We consider a dual EH link, where, at the beginning of a *frame* of duration T_m, the transmitter generates a packet which is to be delivered to the receiver by the end of the frame. In each attempt, the packet transmission is followed by an acknowledgment (ACK) or negative ACK (NACK) signal from the receiver, indicating the success or failure of the attempt, respectively. The ACK and NACK messages are assumed to be received without error and delay [11]–[17], [19], [26]. If an ACK is received, then the packet is not retransmitted,

and both EHNs simply accumulate the harvested energy in a finite capacity battery, till the end of the frame. A packet transmission attempt requires a slot of duration T_p, including the time for reception of the ACK/NACK message. Thus, the packet can be attempted at most $K \triangleq \lfloor T_m/T_p \rfloor$ times in a frame, where $\lfloor . \rfloor$ denotes the floor function. If the packet is not delivered within the K attempts, it is *dropped*.

A. Energy Harvesting Model

In this paper, for clarity of exposition, we start by modeling the EH process at both nodes as a stationary, temporally independent and identically distributed (i.i.d.) Bernoulli process, and independent of each other. That is, at the start of a slot, the transmitting and receiving EHNs independently harvest E_s units of energy with probability ρ_t and ρ_r, respectively, while no energy is harvested with probability $1-\rho_t$ and $1-\rho_r$ [11]–[17]. The Bernoulli model, motivated by switch-based and vibration-based harvesting mechanisms [27], while simple, captures the sporadic and random nature of the EH process. Also, the results obtained using Bernoulli model are amenable for direct extension to more general models such as the stationary Markov model [9], [11] and the generalized Markov model [28], which capture the temporal correlation of the EH processes at the EHNs, and are appropriate to model solar and piezoelectric harvesting processes, respectively [1], [28]. The extension of our proposed design procedure to the case of spatio-temporally correlated EH processes is presented in Sec. VII.

B. Energy Management at the Transmitter and Receiver

The transmit power level for each *attempt* of a given packet is dictated by a *retransmission index-based policy* (RIP) $\mathcal{P} = \{P_1 \triangleq \frac{L_1 E_s}{T_p}, P_2 \triangleq \frac{L_2 E_s}{T_p}, \ldots, P_K \triangleq \frac{L_K E_s}{T_p}\}$, where $L_\ell \in \mathbb{R}^+$, and $L_\ell E_s$ denotes the energy used to make the ℓ^{th} transmission attempt and receive the corresponding ACK/NACK feedback message. The transmit power level in each attempt is constrained by the maximum transmit power allowed by the RF front-end of the system, $\frac{L_{\max} E_s}{T_p}$. That is, $L_\ell \leq L_{\max}$ for all ℓ. The policy $\mathcal{P}$ is an attempt-based power prescription, and not a slot-based prescription. Also, $\mathcal{P}$ is independent of the instantaneous state-of-charge (SoC) at both the transmitter and receiver. This makes the RIPs easier to operate and hence suitable for applications where it is energy-expensive to obtain accurate SoC information.

The receiver consumes RE_s, $R \in \mathbb{R}^+$, units of energy to receive and decode a packet including the energy required to send the ACK/NACK message, as in [16], [20], and [29]. This is reasonable because the modulation and coding scheme remains the same for all attempts.

The policy $\mathcal{P}$ is required to conform to the energy neutrality constraint (ENC), which in turn determines the battery evolution at the EHNs, as follows:

$$B^t_{n+1} = \min(B^t_n + \mathbb{1}_{\{E^t_n \neq 0\}} - L_\ell \mathbb{1}_{\{L_\ell \leq B^t_n, R \leq B^r_n, U_n \neq -1\}}, B^t_{\max}), \tag{1}$$

where B^t_n denotes the battery level in the n^{th} slot at the transmitter, $\mathbb{1}_{\{E^t_n \neq 0\}}$ is an indicator function taking the value 1 if the transmitter harvests energy in the n^{th} slot (which happens with probability ρ_t), and zero otherwise. Note that, throughout the paper, the battery levels such as B^t_n, B^r_n, $B^t_{\max}$, $B^r_{\max}$, are normalized with respect to E_s, where B^r_n and $B^r_{\max}$ denote the state of the battery at the receiver in the n^{th} slot and the receiver battery capacity, respectively. Also, $B^t_{\max}$ denotes the size of the battery at the transmitter, and U_n denotes the *transmission status* of the current packet, defined as

$$U_n \triangleq \begin{cases} -1 & \text{ACK received,} \\ \ell & \ell - 1 \text{ NACKs received, } \ell \in \{1, \ldots, K\}. \end{cases} \tag{2}$$

That is, at the start of the frame, U_n is initialized to 1, and is incremented by one if a NACK is received, and is set equal to -1 once an ACK is received. Thus, (1) captures the fact that the EHNs accumulate the harvested energy for the rest of the frame, after an ACK is received.[1] The battery at the receiver evolves in a manner similar to (1). The energy buffer at the transmitter and receiver are assumed to be perfectly efficient.

In the n^{th} slot, the ℓ^{th} attempt is made if and only if $B^t_n \geq L_\ell$, $B^r_n \geq R$ and $U_n \neq -1$. Otherwise, both nodes go to sleep, and wake up when they have sufficient energy to support the next attempt. This coordination can be achieved using a signaling scheme in which the receiver abstains from sending the ACK/NACK message for the current attempt until it has sufficient energy to receive the next attempt. Further, upon receiving an ACK/NACK message, the transmitter wakes up once it has sufficient energy to make the next attempt [16], [31]. After sending the ACK/NACK message, the receiver senses the channel at the beginning of each slot, and goes to sleep if no transmission is detected. This is an alternate implementation of the coordinated sleep-wake protocol (CSWP) [16], [31]. In contrast to CSWP, this scheme does not require explicit control signaling to communicate the energy availability to the other node.

The system dynamics for three consecutive frames is pictorially illustrated in Fig. 1. The first packet gets delivered in the Ψ_1^{th} attempt, which is made in the last slot, while the second packet is dropped due to channel outage and energy outage at the transmitter. In the third frame, the packet is delivered in the second attempt. Note that, in the third frame, the first attempt is made in the second slot, after the transmitter harvests sufficient energy to make a transmission attempt.

C. Wireless Channel Model

The packet is transmitted over a *block* fading channel, with two cases for the block duration. In the first case, termed *slow* fading, the channel remains constant for all the transmissions

[1] Note that, (1) assumes that the node consumes energy only in communication. The results obtained in this paper can be easily extended to the scenario where, in each slot, a node consumes a constant $L_{on}E_s$ units of energy to remain on and carry out the signal processing tasks, and the amount of energy spent by the node in communication is proportional to the actual transmit power (or the energy required for decoding, RE_s, if it is a receiver), which is the case for nodes with variable bias class-A power amplifiers [30]. In this scenario, (1) modifies as $B^t_{n+1} = \min(B^t_n + \mathbb{1}_{\{E^t_n \neq 0\}} - L_{on} - \frac{L_\ell}{\eta} \mathbb{1}_{\{L_\ell \leq B^t_n, R \leq B^r_n, U_n \neq -1\}}, B^t_{\max})$, where η is the efficiency of the power amplifier. The results in this case can be obtained by accounting for the fact that the energy required for transmission is $\frac{L_\ell E_s}{\eta}$ [8].

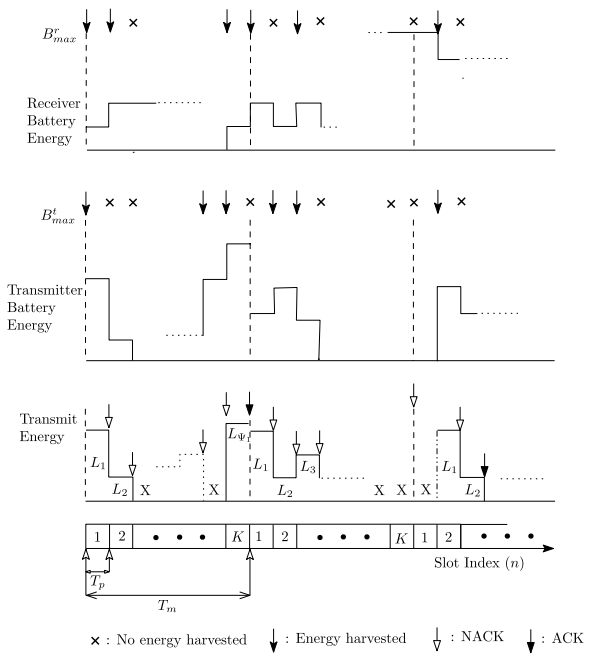

Fig. 1. System dynamics of the dual EH link, showing the random energy harvesting moments (↓) and periodic data arrivals (↑). The marker "X" denotes the slots where no attempt is made due to insufficient energy at the EHN, and Ψ_1 denotes the number of possible attempts. For instance, in a system with $K = 4$, the RIP $\mathcal{P} = [\frac{E_s}{T_p}\ \frac{2E_s}{T_p}\ \frac{3E_s}{T_p}\ \frac{4E_s}{T_p}]$ makes successive attempts using E_s, $2E_s$ units of energy, and so on, provided both the EHNs have sufficient energy for the attempt.

of a given packet and changes in an i.i.d. fashion at the start of a new frame. In the second case, termed *fast* fading, the channel varies from slot to slot in an i.i.d. fashion. The transmitter has only implicit knowledge of the channel state information obtained through the ACK/NACK messages from the receiver. In both slow and fast fading cases, the channel is assumed to be Rayleigh distributed, with the complex baseband channel distributed as $\mathcal{CN}(0, \sigma_c^2)$.

D. Outage Model

We investigate the optimal policy design for two different retransmission protocols at the link layer: the ARQ and the HARQ-CC. In ARQ, a packet received in a given attempt is decoded independently of the packets received in previous failed attempts, while in contrast, for HARQ-CC, all the copies of the packet received in the previous attempts are maximal ratio combined with the current packet, and decoding is performed on the combined output. For ARQ, the packet received in the ℓ^{th} *attempt* is decoded correctly if $\gamma_\ell \geq \gamma_0$, where γ_ℓ is the SNR of the packet received in the ℓ^{th} attempt and γ_0 is the minimum SNR required for successful decoding. Otherwise, the packet is said to be in *outage*. The probability that an outage occurs in the ℓ^{th} attempt is [16], [19], [26]

$$p_{\text{out},\ell} \triangleq \Pr[\gamma_\ell < \gamma_0] = 1 - e^{-\frac{\gamma_0 \mathcal{N}_0}{P_\ell \sigma_c^2}}, \tag{3}$$

where $\mathcal{N}_0$ denotes the power spectral density of the AWGN at the receiver and $\gamma_\ell \triangleq P_\ell |h_\ell|^2 / \mathcal{N}_0$. While for HARQ-CC, an outage occurs if the SNR accumulated up to and including ℓ^{th} attempt, $\gamma_{ac,\ell}$, is less than γ_0. Thus, the outage probability for HARQ-CC is given as

$$p_{\text{out},1\to\ell} \triangleq \Pr[\gamma_{ac,\ell} < \gamma_0], \quad \text{where } \gamma_{ac,\ell} \triangleq \sum_{i=1}^{\ell} \frac{P_i |h_i|^2}{\mathcal{N}_0}, \tag{4}$$

where $|h_\ell|^2$ denotes the channel gain in the ℓ^{th} attempt. Note that, $p_{\text{out},0} = p_{\text{out},1\to 0} = 1$. In addition, for both ARQ and HARQ-CC, a packet remains in outage if either of the EHNs do not have sufficient energy to make an attempt. A packet which remains in outage till the end of the frame is *dropped*.

The goal of this paper is to find an optimal RIP $\mathcal{P}$ for the above described system. The first step in that direction is to obtain an analytical expression for the PDP of the system in terms of the power levels, P_ℓ, of the RIP $\mathcal{P}$. The PDP of the above described system was analyzed in [16] and [17]. In this paper, we use the expressions obtained in the previous work to design PDP-optimal policies. In the next section, we present asymptotically tight upper and lower bounds on the PDP, which, in turn, enable us to design RIPs using tools from GP.

III. Bounds on the PDP

Our starting point is the closed-form PDP expressions obtained in [16] and [17], which we summarize first. The evolution of the dual EH system can be modeled as a discrete-time Markov chain (DTMC) whose state is denoted by the tuple (B_n^t, B_n^r, U_n). The PDP is computed in terms of the conditioned PDP, denoted by $P_{\text{D}}(K|i, j, U_n = 1)$, which is the packet drop probability conditioned on the batteries having (iE_s, jE_s) units of energy at the start of the frame ($U_n = 1$). Thus, using the law of total probability, the PDP is written as

$$P_{\text{D}}(K) = \sum_{(i,j)} \pi(i, j) P_{\text{D}}(K|i, j, U_n = 1), \tag{5}$$

where $\pi(i, j)$ denotes the stationary probability of the event that at the start of the frame, the battery state at the transmitter and receiver is (iE_s, jE_s), with $(i, j) \in \{(i_t, j_r) \mid 0 \leq i_t \leq B^t_{\max}, 0 \leq j_r \leq B^r_{\max}\}$. The stationary probabilities, $\pi(i, j)$, can be obtained by solving the balance equations, $\pi = \pi \text{P}$, where the entries of P are the K-step transition probabilities $\Pr(B^t_{MK} = i_1, B^r_{MK} = j_1 | B^t_{(M-1)K} = i_2, B^r_{(M-1)K} = j_2)$, where M denotes the frame index. The K-step transition probabilities can be computed from the TPM of the DTMC, whose entries, in turn, are obtained by accounting for the harvesting and outage events that could occur in a slot. Explicit expressions for P can be found in [16]. Next, $P_{\text{D}}(K|i, j, U_n = 1)$ in (5) can be written as

$$\begin{aligned} P_{\text{D}}(K|i, j, U_n = 1) = \sum_{m_t=0}^{K} \sum_{m_r=0}^{K} \binom{K}{m_t} \binom{K}{m_r} \rho_t^{m_t} \rho_r^{m_r} \\ \times (1 - \rho_t)^{K - m_t} (1 - \rho_r)^{K - m_r} \\ \times p_{\text{D}}(i, j, m_t, m_r), \end{aligned} \tag{6}$$

where $p_{\text{D}}(i, j, m_t, m_r)$ denotes the PDP conditioned on the batteries at the transmitter and receiver being at states i and j at the start of the frame and harvesting energy in m_t and m_r slots over the frame, respectively, and depends on

the RIP $\mathcal{P}$ and the channel statistics. Expressions for $p_{\mathrm{D}}(i, j, m_t, m_r)$ for slow and fast fading channels with both ARQ and HARQ-CC protocols are provided in [16, Sec. IV]. Now, we proceed to formulate the PDP optimization problem and present our lower and upper bounds on the PDP.

A. Derivation of the Bounds

In this section, we formulate the optimization problem to minimize the PDP. The objective function of this optimization problem is given by (5). The problem of finding the optimal RIPs for dual EH links, subject to the ENC and peak power constraint can be stated as follows:

$$\textbf{(P1)} \quad \min_{\mathcal{P}=\{P_1,\ldots,P_K\}} \sum_{(i,j)\in I} \pi(i,j) P_{\mathrm{D}}(K|i,j,U_n=1), \quad (7)$$

subject to $0 \leq P_\ell \leq P_{\max}$, $1 \leq \ell \leq K$, where $P_{\max} \triangleq \frac{L_{\max} E_s}{T_p}$ and I represents the set of all possible tuples of battery states at the transmitter and receiver. Note that, in the above formulation, the ENC manifests through the stationary probabilities, $\pi(i, j)$, which are determined by the transition probabilities of the DTMC. Due to this, both $\pi(i, j)$ and $P_D(K|i, j, U_n = 1)$ have a complicated dependence on the policy $\mathcal{P}$. Moreover, for moderate to large battery capacities, the large state space involved makes it computationally prohibitive to use dynamic programming based approaches.

To reformulate the problem in a computationally tractable form, we look to simplify both the objective and the constraints of (**P1**), without compromising the optimality of the solution. To this end, we first derive asymptotically tight lower and upper bounds on the PDP. The bounds are motivated by the observation that for all possible tuples (i, j) of the battery state at the start of the frame for which the EHNs have sufficient energy to make all K attempts irrespective of the amount of energy harvested during the frame (m_t and m_r), the conditional PDP, $P_{\mathrm{D}}(K|i, j, U_n = 1)$, is the same. This is because, for all such battery state tuples (i, j), $p_{\mathrm{D}}(i, j, m_t, m_r)$ is equal to the probability that the packet remains in outage after the K attempts, for all m_t and m_r. The bounds are obtained by recognizing that the PDP when all K attempts cannot be guaranteed is at least equal to the PDP when all K attempts can be made, and is at most equal to 1. The next Lemma provides a lower and an upper bound on the PDP.

Lemma 1: Consider a dual EH link operating with an RIP $\mathcal{P}$ such that $L_\ell \leq L_{\max}$ for all $1 \leq \ell \leq K$. Let I_1 and I_2 be a partition of the set I of tuples of battery states at the transmitter and receiver such that $I_1 \triangleq \{(i, j)|0 \leq i < KL_{\max} < B^t_{\max}$, and $0 \leq j < KR < B^r_{\max}\}$, and $I_2 \triangleq I \backslash I_1$. Then,

$$P^*_{D_\infty} \leq \min_{\mathcal{P}} \sum_{(i,j)\in I} \pi(i,j) P_D(K|i,j,U_n=1) \leq P^*_{D_\infty} + \sum_{(i_1,j_1)\in I_1} \pi(i_1,j_1)\big|_{\mathcal{P}^*},$$

where $P^*_{D_\infty} \triangleq \min_{\mathcal{P}} P_D(K|i, j, U_n = 1)$ and $\mathcal{P}^* \triangleq \arg\min_{\mathcal{P}} P_D(K|i, j, U_n = 1)$, both subject to $(i, j) \in I_2$.

Proof: See Appendix A. ∎

Thus, the PDP of a dual EH link with finite sized batteries is lower bounded by $P^*_{D_\infty}$, the minimum conditional PDP that can be obtained when all K attempts are feasible. The lower bound is also the optimum PDP with infinite size batteries. This is because the optimum policy with infinite size batteries is the one that minimizes the PDP among all policies for which the average energy consumed is less than or equal to the average energy harvested at both nodes [7]. A link satisfying this constraint is said to operate in the *energy unconstrained regime* (EUR) [16, Sec. V]. Under EUR, the policy will induce a positive drift in the battery level of both EHNs, which ensures that the nodes will eventually always be able to make all K attempts. On the other hand, the upper bound indicates that the optimal policy will try to minimize the stationary probability of the set I_1, i.e., the set of the battery states where all K attempts are not guaranteed. Hence, the optimal policy will induce a drift away from the set I_1, which, in turn, also implies a positive drift on the battery states. In the next section, we show that for the policies which induce a positive drift, the bounds proposed in Lemma 1 are tight, provided the battery sizes are sufficiently large. This allows us to approximate the objective function with the lower bound as well as to replace the ENC with a more amenable average power constraint.

IV. Tightness of the Bounds in the EUR

In the following, we establish that, in the EUR, the bounds presented in Lemma 1 are asymptotically tight. It is shown that the difference between the bounds goes to zero as the sum of two terms, each of which decays exponentially with the battery size at the transmitter and receiver, respectively. We first present the following Lemma for the transmitter of a dual EH link.

Lemma 2: Consider the transmitter of a dual EH link operating in the EUR with an RIP $\mathcal{P}$ such that $L_\ell \leq L_{\max}$ for all $1 \leq \ell \leq K$. The stationary probability of the battery at the transmitter being in a state $i \in I^t_1 \triangleq \{i : 0 \leq i < KL_{\max} < B^t_{\max}\}$, such that the transmitter cannot support all K attempts, decays exponentially with $B^t_{\max}$, i.e., $\sum_{i\in I^t_1} \boldsymbol{\pi}_t(i) = \Theta(e^{r^t_* B^t_{\max}})$, where $\boldsymbol{\pi}_t$ denotes the stationary distribution of the battery states at the transmitter and r^t_* is the negative root of the asymptotic log moment generating function (MGF) of the drift process $X^t_n \triangleq \mathbb{1}_{\{E^t_n \neq 0\}} - \mathcal{L}(B^t_n, B^r_n, U_n)$. Here, $\mathbb{1}_{\{E^t_n\neq 0\}}$ is the indicator variable which equals one if the transmitter harvests the energy in the n^{th} slot, and zero otherwise, while $\mathcal{L}(B^t_n, B^r_n, U_n)$ denotes the energy used by the RIP in the n^{th} slot. The asymptotic log MGF is defined as $\Lambda(r) \triangleq \lim_{N\to\infty} \frac{1}{N} \log \mathbb{E}\left[\exp\left(r \sum_{n=1}^N X^t_n\right)\right]$, where $r \in \mathbb{R}$.

Proof: See Appendix B. ∎

Qualitatively, when the EHN operates in the EUR, the battery eventually becomes full and makes small excursions from the state $B^t_{\max}$ towards depleting the battery. Whenever the battery is not full, the drift becomes positive, and this drives the battery towards the full state. Hence, for an EHN with a large battery, the event of hitting the set I^t_1 is a large deviation event, which occurs with the accumulation of a number of rare events (for example, when there is a long patch of slots where no energy is harvested). Intuitively, a similar

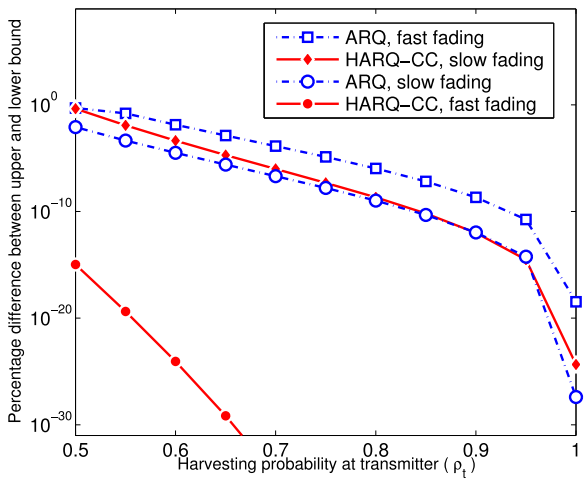

Fig. 2. Difference between the lower bound and upper bounds on the objective function in (**P1**). The parameters chosen are $E_s = 5$ dB, $\gamma_0 = 10$ dB, $\rho_r = 0.9$, $R = 1$, $B^t_{\max} = B^r_{\max} = 25$ and $K = 4$. The policy used is $\left[\frac{E_s}{T_p}\ \frac{E_s}{T_p}\ \frac{2E_s}{T_p}\ \frac{2E_s}{T_p}\right]$. Note that, the nodes operate in the EUR under this policy.

argument holds for both nodes of a link operating in the EUR. Next, we use the above Lemma to substantiate this intuition via the following theorem.

Theorem 1: For a dual EH link employing an RIP which satisfies the peak power constraint and operates in the EUR, $\sum_{(i,j)\in I_1} \boldsymbol{\pi}(i,j) = \Theta(e^{r^t_* B^t_{\max}}) + \Theta(e^{r^r_* B^r_{\max}})$*, where* r^t_* *and* r^r_* *are the negative root of the asymptotic log MGF of the drift process at the transmitter* ($X^t_n \triangleq \mathbb{1}_{\{E^t_n \neq 0\}} - \mathcal{L}(B^t_n, B^r_n, U_n)$) *and receiver* ($X^r_n \triangleq \mathbb{1}_{\{E^r_n \neq 0\}} - \mathcal{R}(B^t_n, B^r_n, U_n)$)*, respectively. Here,* $\mathbb{1}_{\{E^t_n \neq 0\}}$ *or* $\mathbb{1}_{\{E^r_n \neq 0\}}$ *equal one if the energy is harvested at the transmitter or receiver in the* n^{th} *slot, respectively, and zero otherwise. Also,* $\mathcal{L}(B^t_n, B^r_n, U_n)$ *and* $\mathcal{R}(B^t_n, B^r_n, U_n)$ *denote the amount of energy used in the* n^{th} *slot at the transmitter and receiver, respectively.*

Proof: See Appendix D. ∎

The above result establishes that for dual EH links operating in the EUR, $\sum_{I_1} \boldsymbol{\pi}(i,j)$ decreases exponentially with the size of the battery at the transmitter and receiver. In Fig. 2, we illustrate that for a dual EH link operating in the EUR and equipped with moderate sized energy buffers, the percentage difference between the lower and upper bounds on the objective function is negligible. Thus, the lower bound in Lemma 1 is a close approximation to the objective function in **(P1)**. Furthermore, the above result implies that the energy neutrality constraint in **(P1)** can be replaced by the simpler EUR constraint, without compromising on the optimality. We conclude this section with the following observation.

Remark 1: As shown in [25, Lemma 3], for a policy with a drift δ (the difference between the mean energy harvested and the mean energy consumed) the negative root of the asymptotic log MGF of the resulting drift process is equal to $-\frac{2\delta}{\sigma_e^2} + o(\delta)$, where σ_e^2 is the asymptotic variance [25] of the harvesting process. Thus, for the processes X^t_n and X^r_n, the negative roots r^t_* and r^r_* are of the order of the energy saved per frame at the transmitter and receiver, respectively. Thus, for a smaller drift, a larger battery would be needed to achieve the same performance (See Fig. 3). Furthermore, for a given drift δ, the harvesting process with larger asymptotic variance, σ_e^2, would require a larger battery.

In the next section, we reformulate **(P1)** using the result obtained in Theorem 1.

V. Problem Reformulation

In this section, we design RIPs under the EUR constraints, and then choose the battery size according to Theorem 1.[2]

Under Theorem 1, we can reformulate the problem **(P1)** by choosing the lower bound, i.e., $P_{\mathrm{D}}(K|i,j,U_n=1)$ with $(i,j) \in I_2$, as the objective function, and by replacing the ENC by the EUR constraints. Using (6), as a node operating in the EUR can make all K attempts, $P_{\mathrm{D}}(K|i,j,U_n=1) = p_{\mathrm{D}}(i,j,m_t,m_r) = f(\mathcal{P})$ for all $(i,j) \in I_2$, irrespective of the number of slots (m_t and m_r), in which energy is harvested. Therefore, in general, for a dual EH link operating in the EUR, the PDP minimization problem is written as follows:

$$\min_{\bar{\mathbf{L}}=\{L_1,\ldots,L_K\}} \quad p_{\mathrm{D}}(i,j,m_t,m_r), \tag{8a}$$

$$\text{subject to} \sum_{\ell=1}^{K} L_\ell \ p_{\mathrm{o},\ell-1} \leq K\rho_t, \tag{8b}$$

$$\sum_{\ell=1}^{K} \chi^\ell p_{\mathrm{o},\ell-1} \leq \frac{K\rho_r}{R}, \tag{8c}$$

and $0 \leq L_i \leq L_{\max}$, $1 \leq i \leq K$, where $\chi^\ell \triangleq \mathbb{1}_{\{L_\ell \neq 0\}}$ is an indicator variable which is $= 1$ if $L_\ell \neq 0$ and $= 0$ otherwise, and $p_{\mathrm{o},\ell-1}$ denotes the probability that the first $\ell-1$ transmission attempts have failed; $p_{\mathrm{o},0} = 1$. In the above, (8b) and (8c) are the EUR constraints. For example, (8b) is written using the fact that the transmitter operates in the EUR if the average energy consumed by it, $\sum_{\ell=1}^{K} L_\ell E_s p_{\mathrm{o},\ell-1}$, is less than the average energy harvested, $K\rho_t E_s$. The average energy consumed is computed using the fact that ℓ^{th} attempt is made only if all the previous $\ell-1$ attempts have failed, which happens with probability $p_{\mathrm{o},\ell-1}$, where $p_{o,\ell-1}$ can be written in terms of the outage probabilities defined in (3) and (4). The receiver operates in the EUR when a similar condition is satisfied. In (8c), χ^ℓ denotes the fact that the receiver consumes R units of energy only if the transmitter makes an attempt at a nonzero power level.

The solution of (8) provides an RIP which achieves near-optimal PDP for the EHNs equipped with batteries of size as prescribed by Theorem 1.

Note that, due to the indicator variables χ^ℓ in the formulation, the optimization problem (8) is of exponential complexity in K, the number of attempts allowed. In the next subsection,

[2]The typical battery size for practical EHNs ranges between 200 mAh-2500 mAh [32]. A 200 mAh capacity battery can deliver 720 J of energy at a nominal voltage of 1 V. Also, using a small solar panel, at 66% efficiency, NiMH batteries receive 0.13 mJ of energy per 10 ms slot. Thus, with two hours of sunlight, the typical battery size, normalized with respect to E_s, equals 5.33×10^6. Hence, the large battery size assumption is reasonable.

we discuss an interesting observation which reduces the computational complexity from being exponential to linear in the number of attempts.

A. Simplification of Integer Constraints

The problem (8) is essentially a set of $2^K - 1$ problems. Depending on the values taken by the variables χ^ℓ, the feasibility set of each problem changes. For a given value of the variables $\{\chi^\ell\}_{\ell=1}^K$, the objective and constraints in (8) are nonconvex functions, and hence, each individual subproblem is a nonconvex nonlinear program. Thus, (8) is a nonconvex mixed integer nonlinear program (NMINLP). In general, finding the solution of an NMINLP is a strongly NP-hard problem [33]. Hence, in order to solve (8), we need to solve $2^K - 1$ subproblems, and choose the solution of the subproblem which gives minimum objective value among them as the solution to (8). However, we observe that the solution of (8) only depends on $\chi = \sum_{\ell=1}^K \chi_\ell$, i.e., if χ is same for two subproblems then both will have the same minimum. This observation leads to a simplification that, to find a solution to (8), we need to solve only K nonconvex nonlinear subproblems corresponding to the different possible values of χ, and pick the solution of the subproblem which results in the minimum objective value among them. Thus, the number of subproblems that need to be solved becomes linear rather than exponential in K. One approach to solving these K subproblems is to use standard non-convex problem solvers such as interior point methods. However, such techniques may not be computationally feasible to implement as the problem dimension gets large. Hence, in this paper, we adopt a computationally efficient approach based on GP, to arrive at the optimal solution in a numerically stable manner.

In the next section, we present a method to find near-optimal RIPs for both ARQ and HARQ-CC based dual EH link with slow and fast fading channels.

VI. Near-Optimal RIPs for Dual EH Links

A. Dual EH Links With ARQ and Fast Fading

In this subsection, we find near-optimal policies for a dual EH link with ARQ and fast fading channels. Using the expression for $p_{\mathrm{D}}(i, j, m_t, m_r)$ given in [16, Lemma 6] and EUR constraints in [16, Sec. V], the PDP optimization problem can be written as

$$\min_{\tilde{\mathbf{L}}=\{L_1,\ldots,L_K\}} \prod_{\ell=1}^{K}\left(1-e^{-\frac{s}{L_\ell}}\right), \tag{9a}$$

$$\text{subject to } \sum_{\ell=1}^{K} L_\ell \prod_{i=1}^{\ell-1}\left(1-e^{-\frac{s}{L_i}}\right) \le K\rho_t, \tag{9b}$$

$$\sum_{\ell=1}^{K} \chi^\ell \prod_{i=1}^{\ell-1}\left(1-e^{-\frac{s}{L_i}}\right) \le \frac{K\rho_r}{R}, \tag{9c}$$

and $0 \le L_\ell \le L_{\max}$, $\chi^\ell \in \{0,1\}$, $1 \le \ell \le K$, where $s \triangleq \frac{\gamma_0 \aleph T_p}{E_s \sigma_c^2}$. The constraints in (9b) and (9c) ensure that both the transmitter and receiver operate in the EUR. As discussed above, to solve (9), we need to solve K subproblems, and pick the best among the resulting solutions. Hence, in the following, we focus on solving an individual subproblem, which is a nonconvex nonlinear program. We first convert the problem into a *complementary geometric* program (CGP) [34], as follows. Specifically, for $\chi = K'$, using the Taylor series expansion of e^{-x}, (9) can be rewritten as

$$\min_{\tilde{\mathbf{Z}}=\{t,Z_1,\ldots,Z_{K'}\}} t,$$

$$\text{subject to } \prod_{\ell=1}^{K'}(A_\ell - B_\ell) \le t, \tag{10a}$$

$$\frac{Z_1^{-1} + Z_2^{-1}A_1 + Z_3^{-1}(A_1A_2 + B_1B_2) + \cdots}{\frac{K\rho_t}{s} + Z_2^{-1}B_1 + Z_3^{-1}(A_1B_2 + A_2B_1) + \cdots} \le 1, \tag{10b}$$

$$\frac{1 + A_1 + A_1A_2 + B_1B_2 + \cdots}{\frac{K\rho_r}{R} + B_1 + (A_1B_2 + A_2B_1) + \cdots} \le 1, \tag{10c}$$

and $0 \le sZ_\ell^{-1} \le L_{\max}$, $1 \le \ell \le K'$, where $A_\ell \triangleq \sum_{i=0}^{\infty} \frac{Z_\ell^{2i+1}}{(2i+1)!}$, $B_\ell \triangleq \sum_{i=1}^{\infty} \frac{Z_\ell^{2i}}{(2i)!}$, and $Z_\ell \triangleq \frac{s}{L_\ell}$. In the above problem, A_ℓ and B_ℓ are infinite summations. First, we construct a finite (say, 5th) order approximation of the infinite summations involved. It is worth mentioning that the loss in optimality in making this approximation has a negligible effect on the performance, when one considers 5 or 7 terms in the expansion. The resulting finite order approximation of the constraints in (10a), (10b) and (10c) are ratios of posynomials, which are nonconvex, and hence (10) is a CGP which is an intractable NP-hard problem [34]. Since directly solving (10) is hard, we solve it by solving a series of approximations, each of which can be easily solved optimally. Specifically, using a result in [34, Lemma 1], we approximate the denominators of (10a), (10b) and (10c) with monomials. This results in a *geometric* program (GP) approximation of (10), which can be solved efficiently and optimally.

The monomial approximation for a posynomial is constructed as follows. Let $g(\mathbf{x}) = \sum_i v_i(\mathbf{x})$ be a posynomial, with $v_i(\mathbf{x})$ being monomials (which are nonnegative by definition), then

$$g(\mathbf{x}) \ge \tilde{g}(\mathbf{x}) \triangleq \prod_i \left(\frac{v_i(\mathbf{x})}{\beta_i}\right)^{\beta_i}, \tag{11}$$

where $\beta_i \triangleq \frac{v_i(\mathbf{x}_0)}{g(\mathbf{x}_0)}, \forall\, i$, (and note that $0 \le \beta_i \le 1$), for any fixed $\mathbf{x}_0 > 0$. Then $\tilde{g}(\mathbf{x}_0) = g(\mathbf{x}_0)$, and $\tilde{g}(\mathbf{x})$ is the best local monomial approximation to $g(\mathbf{x})$ near $\mathbf{x_0}$ in the sense of the first order Taylor approximation [34].

We solve (10) iteratively. In the p^{th} iteration, we use the GP approximation in (11), with the coefficients β_i computed by evaluating the denominator posynomials in (10a), (10b) and (10c) at $\mathbf{Z}^{(p)}$, the solution of the $(p-1)^{\text{th}}$ iteration. The procedure is summarized in Algorithm 1.

It can be shown that Algorithm 1 converges to a point which satisfies the Karush-Kuhn-Tucker (KKT) conditions of the original problem [34]. In the sequel, we show, through simulations, that it actually converges to a point at which the objective function is very close to the global optimum.

Algorithm 1 Solution to the Complementary GP

Initialize: $\mathbf{Z}^{(1)} = \{Z_1, Z_2, \ldots, Z_{K'}, 0, \ldots, 0\}$, where $\mathbf{Z}^{(1)}$ is any feasible vector for (10). $p \leftarrow 1$.
do
1) Evaluate the denominator posynomials $G_a(\mathbf{Z})$, $G_b(\mathbf{Z})$ and $G_c(\mathbf{Z})$ in (10a), (10b) and (10c), respectively, with the given $\mathbf{Z}^{(p)}$.
2) For each term V_ℓ^q in the denominator posynomials $G_q(\mathbf{Z})$, where $q = a, b$ and c, compute $\beta_\ell^q = \frac{V_\ell^q(\mathbf{Z}^{(p)})}{G_q(\mathbf{Z}^{(p)})}$.
3) Replace the denominator posynomial of (10a), (10b) and (10c) with a monomial using (11), with the weights β_ℓ^q.
4) Solve the GP (e.g., using GGPLAB [35]) to obtain $\mathbf{Z}^{(p+1)}$; set $p \leftarrow p + 1$.
5) Go to step 1, and use $\mathbf{Z}^{(p)}$ obtained in step 4.

while $\|\mathbf{Z}^{(p+1)} - \mathbf{Z}^{(p)}\|_2 \leq \epsilon$.
Output: The near-optimal RIP and PDP are given by $\mathbf{Z}^{(p+1)}$ and t, respectively.

This substantiates our use of GP techniques, specifically Algorithm 1, to solve the problem (10) in a provably convergent manner.

B. Design of Optimal Policies for Other Cases

The problems of finding optimal policies for dual EH links for slow fading channels with ARQ and HARQ-CC as well as for fast fading channels with HARQ-CC are solved similarly, and the details are presented in Appendices E and F, respectively.

Remark 2: The results presented in this section can also be used to design the RIPs for mono EH links, by dropping the constraint corresponding to the non-EH node.

In the following section, we extend the presented design to a scenario when the EH processes at both nodes are spatially and temporally correlated.

VII. Spatio-Temporally Correlated EH Processes

A. Temporal Correlation

In this section, to account for the temporal correlation, we assume that the EH processes at both nodes can be modeled as a first-order stationary Markov chain [1], [28]. The harvesting process at the transmitter is described by the set of harvesting energy levels, $\mathcal{E} = \{e_1^t, \ldots, e_{\max}^t\}$, and the probabilities, $p_{a,b} = \Pr[E_{n+1}^t = e_a^t | E_n^t = e_b^t]$, that in the $(n+1)^{\text{th}}$ slot the transmitter harvests e_a^t units of energy, given that it harvested e_b^t units of energy in n^{th} slot, where both e_a^t and $e_b^t \in \mathcal{E}$. The harvesting process at the receiver is modeled similarly. First, we present the expressions for the PDP of dual EH links with stationary Markov EH process at the transmitter and receiver, obtained in [16, Sec. VII A]:

$$P_{\mathrm{D}}(K) = \sum_{(i,j,e_a^t,e_c^r)} \pi(i, j, e_a^t, e_c^r) P_{\mathrm{D}}(K|i, j, e_a^t, e_c^r, U_n = 1), \tag{12}$$

where $\pi(i, j, e_a^t, e_c^r)$ denotes the stationary probability that at the beginning of the frame, the state of the battery and the EH process at the transmitter and receiver are (i, j) and (e_a^t, e_c^r), respectively. Also, $P_{\mathrm{D}}(K|i, j, e_a^t, e_c^r, U_n = 1)$ denotes the PDP conditioned on the state at the beginning of the frame, and is computed as follows

$$P_{\mathrm{D}}(K|i, j, e_a^t, e_c^r, U_n = 1) = \sum_{E_t=0}^{K e_{\max}^t} \sum_{E_r=0}^{K e_{\max}^r} p(E_t, E_r | e_a^t, e_c^r) \times p_{\mathrm{D}}(i, j, E_t, E_r). \tag{13}$$

In the above, $p(E_t, E_r|e_a^t, e_c^r)$ denotes the probability that the transmitter and receiver harvest E_t and E_r units of energy during the frame, given that they started with e_a^t and e_c^r units of energy, respectively, at the start of the frame. In (13), $p_{\mathrm{D}}(i, j, E_t, E_r)$ denotes the packet drop probability when the batteries are in state (i, j) at the start of the frame and the nodes harvest (E_t, E_r) units of energy during the frame. Next, the PDP in (12) can be rewritten as

$$\begin{aligned} &P_{\mathrm{D}}(K) \\ &= \sum_{(i,j)} \pi(i, j) \sum_{(e_a^t, e_c^r)} \pi(e_a^t, e_c^r | i, j) P_{\mathrm{D}}(K|i, j, e_a^t, e_c^r, U_n = 1), \\ &= \sum_{(i,j)} \pi(i, j) P_{\mathrm{D}}(K|i, j, U_n = 1), \end{aligned} \tag{14}$$

where

$$P_{\mathrm{D}}(K|i, j, U_n = 1) \triangleq \sum_{(e_a^t, e_c^r)} \pi(e_a^t, e_c^r | i, j) \times P_{\mathrm{D}}(K|i, j, e_a^t, e_c^r, U_n = 1).$$

The goal of the RIP design problem is to minimize the PDP in (14) subject to energy neutrality and peak power constraints. Although the objective function in this problem has same expression as in problem (P1), the stationary probabilities, $\pi(i, j)$, are different. Nonetheless, as shown in Appendix G, Theorem 1 is applicable in this scenario also. For dual EH links operating in the EUR, this allows us to replace the objective function by the lower bound $P_{\mathrm{D}}(K|(i, j) \in \mathcal{I}_2, U_n = 1)$ and the energy neutrality constraints by the EUR constraints. Using the definition of the set $\mathcal{I}_2$, (13), and the definition of $P_{\mathrm{D}}(K|i, j, U_n = 1)$ given above, we get $P_{\mathrm{D}}(K|(i, j) \in \mathcal{I}_2, U_n = 1) = p_{\mathrm{D}}(i, j, E_t, E_r)$, where, for ARQ-based slow fading links operating with a strictly increasing policy, $p_{\mathrm{D}}(i, j, E_t, E_r) = p_{\mathrm{out},K}$. Hence, in all cases, $p_{\mathrm{D}}(i, j, E_t, E_r)$ is the probability that the packet remains in outage after making all K attempts [16].

Thus, the optimization problem of finding an optimal RIP in the EUR is obtained from problem (9), (30), (31) and (32) by replacing the $K\rho_t E_s$ and $K\rho_r E_s$ with $K\bar{E}_t$ and $K\bar{E}_r$, respectively. Here, $\bar{E}_t$ and $\bar{E}_r$ denote the mean harvesting rates at the transmitter and receiver. Note that, even with modified EUR constraints, the expressions for the objective and the constraints remain the same, and hence, Algorithm 1 yields a near-optimal RIP. This completes the discussion on RIPs for temporally correlated EH processes.

B. Spatial Correlation

In case the Bernoulli EH process of the transmitter and receiver are correlated, the joint distribution of the harvesting

processes can be modeled as [11], [16]

$$p(e_t, e_r) = p_{00}(1-e_t)(1-e_r) + p_{01}(1-e_t)e_r + p_{10}e_t(1-e_r) + p_{11}e_te_r,$$

where $e_t, e_r \in \{0, 1\}$ are random variables taking nonzero value if energy is harvested at the transmitter and receiver, respectively, and p_{00}, p_{01}, p_{10}, and p_{11} are probability values that add up to 1. In this case, the PDP is given by (5). Further, the conditional PDP for the spatially correlated case is written as [16, Sec. VII-B]

$$P_{\mathrm{D}}(K|i, j, \ell = 1) = \sum_{m_t=0}^{K}\sum_{m_r=0}^{K} p'(m_t, m_r)p_{\mathrm{D}}(i, j, m_t, m_r), \tag{15}$$

where $p'(m_t, m_r)$ denotes the probability that the transmitter and receiver harvest energy in exactly m_t and m_r slots, respectively.

Note that, since the result in Theorem 1 is directly applicable in this scenario, the problem to find optimal RIPs can be formulated by using conditional PDP in (15) as the objective when $(i, j) \in \mathcal{I}_2$. The EUR constraints are written by replacing the $\rho_t E_s$ and $\rho_r E_s$ in (9a) and (9b), respectively, by $(p_{10} + p_{11})E_s$ and $(p_{01} + p_{11})E_s$. The resulting optimization problem is solved using Algorithm 1.

In the next section, we evaluate the performance of the designed RIPs and benchmark them against the state-of-the-art policies. We also validate the results obtained in Sec. IV.

VIII. Numerical Results

A. Simulation Setup

We consider a ZigBee system with carrier frequency 950 MHz and four slots per frame, with a slot duration of $T_p = 100$ ms [36]. The transmitter and receiver are $d = 10d_0$ distance apart, where $d_0 = 10$ m is the reference distance. The path loss exponent is $\eta = 4$. The additive noise corresponds to a bandwidth of 2 MHz and temperature $T = 300\ K$. For this system, $E_s = 5$ dB corresponds to 100 μJ. This is a typical amount harvested from indoor illumination, with a harvester of size 10 cm^2 [1]. Note that, due to the time-diversity offered by fast fading channels, the same value of the PDP can be achieved at significantly lower harvesting levels when the channel is fast fading compared to when it is slow fading [16]. Hence, we use $E_s = 12$ dB and $\gamma_0 = 10$ dB for slow fading channels, and $E_s = 5$ dB and $\gamma_0 = 12$ dB for fast fading channels, to obtain the PDP values in a meaningful range (10^{-2} to 10^{-4}) [26]. This also allows us to show performance under the two channel models in the same plot.

Note that, for short distance communications, the energy consumed by the transmitter and receiver are of the same order [37]. Hence, in each experiment, we set $1 \leq R \leq 1.5$. The size of the battery at the transmitter and receiver is determined using Theorem 1. The channel from the transmitter to the receiver is assumed to be i.i.d. Rayleigh block fading which remains constant for a slot (frame) for the fast (slow) fading channel. In all the experiments, the PDP is computed by averaging over 10^7 frames.

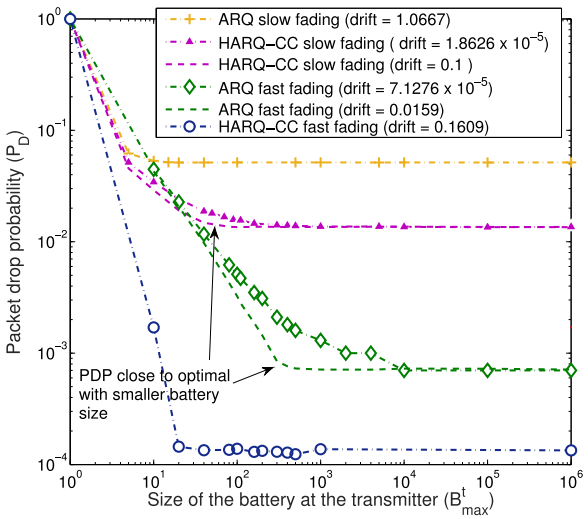

Fig. 3. PDP of dual EH links with finite size batteries asymptotically goes to the PDP of dual EH link with infinite size batteries. The rate of convergence is determined by the drift induced by the policy, i.e., the larger the drift, the faster the convergence. The parameter values are $R = 1$, $\rho_t = 0.75$, $\rho_r = 0.8$ and $L_{\max} = 3$. For HARQ-CC with fast fading channels, $L_{\max} = 2$. The size of the battery at the receiver is the same as the size of the battery at transmitter. The drift induced by a policy is equal to the average of the difference between the energy consumed and the energy harvested in a frame.

B. Results

1) Battery Size Required to Achieve the Lower Bound on the PDP: In Fig. 3, we illustrate the size of the battery required to meet the PDP achieved under infinite-capacity batteries. The policies used in this experiment are designed using Algorithm 1. In all the cases, we observe that the PDP obtained with finite capacity batteries is very close to the lower bound (PDP obtained with a battery size of 10^6), e.g., for ARQ over slow fading channels, the lower bound is achieved when the buffer size exceeds 40 at both the EHNs. In contrast, for ARQ-based fast fading links, the size of the battery required is 10^4. This is because, as noted in Remark 1, the exponents in Theorem 1, r_*^t and r_*^r, are of the order of the drift induced by the RIP. When the drift is low, the system takes a long time to come out of a bad battery state, and therefore, a larger battery size is required to ensure that the probability of hitting a bad state is sufficiently low. For instance, as shown in the figure, in case of ARQ over fast fading channels, the required battery size to achieve near-optimal performance reduces from 10^4 to 10^2 when the drift induced by the RIP increases from 7.1276×10^{-5} to 0.0159. Similar behavior can be observed for HARQ-CC, in slow fading scenarios. Due to this, for ARQ with slow fading channels, a smaller sized energy buffer is required to meet the lower bound compared to ARQ with fast fading channels. This validates the result obtained in Theorem 1 for the required battery capacity.

2) Performance of Proposed RIPs: The results in Fig. 4a show the performance of the proposed policies for ARQ and HARQ-CC with slow fading channels. The performance of the policies matches with that obtained by solving K subproblems using an interior point method (IPM). In addition, compared to the equal power scheme [13], for ARQ-based links, there is an approximately tenfold reduction in the PDP. Similar performance improvement is observed in the proposed policy

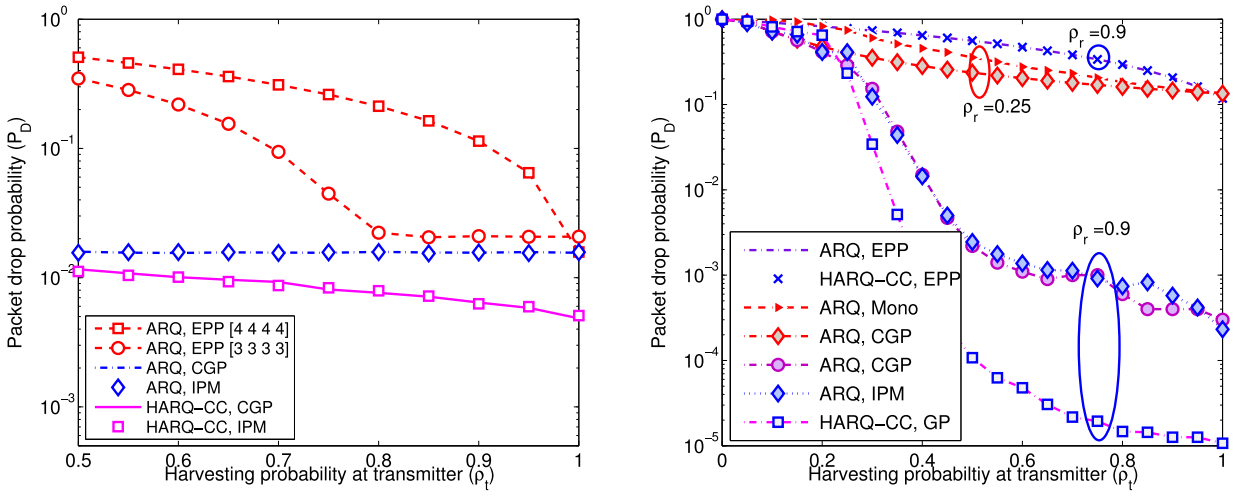

(a) Slow fading channels

(b) Fast fading channels

Fig. 4. For slow fading channels, the performance is compared with the equal power policies (EPP) as well as with the policies obtained using interior point method (IPM). The parameters used: $B^t_{\max} = B^r_{\max} = 40$, $\rho_r = 0.9$, $R = 1$, $L_{\max} = 4$. For fast fading channels, the performance is compared relative to the EPP [4 4 4 4]. The size of energy buffers are $B^t_{\max} = B^r_{\max} = 1000$. In addition, for $\rho_r = 0.25$, the performance of the proposed policy is compared against a policy designed ignoring the harvesting constraint at the receiver. (a) Slow fading channels. (b) Fast fading channels.

over the equal power scheme for the HARQ-CC based links also; we omit the plot to avoid repetition.

The results in Fig. 4b compare the performance of the proposed policies over fast fading channels. In the case of ARQ, to solve the CGP, we approximate the infinite summations by their first three terms only, which leads to a computationally inexpensive optimization procedure, which, nonetheless, matches with the performance obtained using the IPM. For HARQ-CC, the RIPs are obtained by solving a GP, which can be solved efficiently by directly converting it into a convex program. In this case, solving the GP directly using IPM is inefficient. Hence, for HARQ-CC, we omit the comparison with IPM. We observe that, compared to ARQ, HARQ-CC offers an approximately tenfold improvement in the PDP. Also, the equal power policy with transmit power level $4E_s$ performs poorly compared to the designed RIPs. In addition, we compare the performance of the proposed RIP against a policy obtained by solving an optimization problem formulated ignoring the harvesting constraint at the receiver. Note that, for this case, we consider $\rho_r = 0.25$ which corresponds to a scenario when the receiver is energy constrained. The results for this scenario show that it is suboptimal to ignore the harvesting constraint at the receiver.

In Fig. 5, we compare the performance of the proposed RIP designed for ARQ with fast fading channels, against the joint threshold based policy (JTBP), which is essentially an equal power policy with its transmit power level optimized using a global search algorithm [11]. It can be seen that the RIP outperforms both the JTBP and linear policy. This is because the JTBP and linear policy, although simple to implement, are suboptimal. Moreover, the computational complexity of the global search method used to optimize the transmit power levels increases with the buffer size, which is prohibitively large even for moderate sized energy buffers. For example, with $B^t_{\max} = B^r_{\max} = 35E_s$, the size of the search space is approximately 10^8.

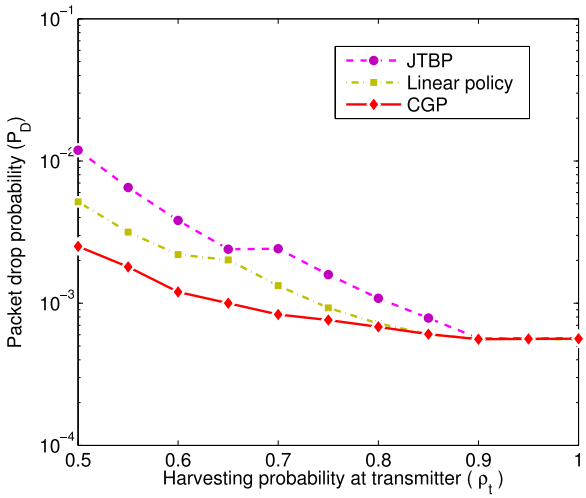

Fig. 5. Performance comparison against the joint threshold based policy (JTBP) and linear policy [11]. The parameters are $R = 1.25$, $\rho_r = 0.7$, $B^t_{\max} = 4000$ and $B^r_{\max} = 500$.

3) Impact of Decoding Energy R: In Fig. 6, we study the impact of energy required for decoding, RE_s. For this experiment, we consider an energy constrained receiver, i.e., the energy required for decoding a packet is close to the average energy harvested by the receiver, in a frame. Also, the receiver has a small battery. We consider two scenarios when the receiver consumes 15 and 20 μJ for maximal ratio combining the packet. Thus, the total energy required for decoding a packet in these scenarios are $1.15E_s$ and $1.2E_s$, respectively. Note that, in these scenarios, the receiver can only support two or one attempts in a frame, on average, respectively, and it is unable to fully exploit the benefits of chase combining. Due to this, in contrast to conventional communication system where HARQ-CC results in improved performance, the ARQ outperforms the HARQ-CC. Also observe that, for $\rho_t > 0.4$, the PDP improves with decrease in R. This is because, for

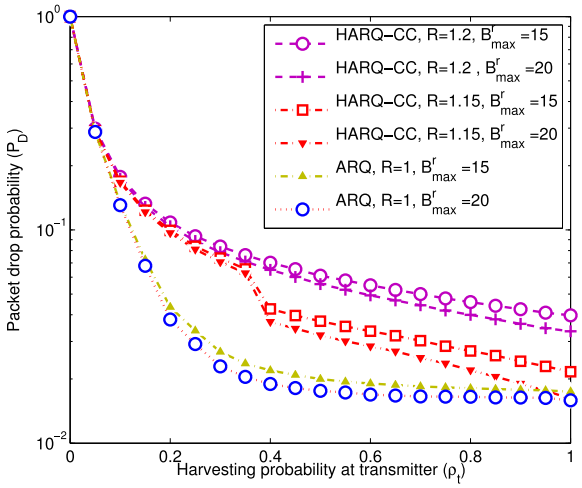

Fig. 6. Impact of decoding energy: ARQ outperforms HARQ-CC when the receiver is energy constrained and the energy cost of combining packets is nonzero. The parameters used are $B^t_{\max} = 20$, $\rho_r = 0.3$ and $L_{\max} = 4$.

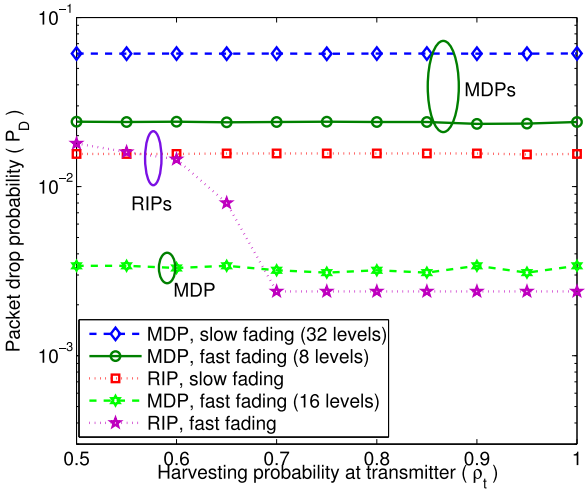

Fig. 7. Performance comparison of RIPs for ARQ based mono-T links with policies designed using an MDP approach assuming access to perfect SoC information [14]. For slow fading channels, the proposed RIP uniformly outperforms the MDP, while in the fast fading case, for $\rho_t \geq 0.7$, the RIPs outperform the corresponding MDP based policies. The parameters used are $B^t_{\max} = 40$ and $L_{\max} = 4$ and 2 for slow and fast fading channels, respectively.

$R = 1.15$, the receiver can support two attempts, while for $R = 1.2$, it can support only one attempt on average. Also, it is easy to observe that we can trade off R for ρ_r. However, once the receiver has sufficient energy to support all K attempts, the decrease in R (or increase in ρ_r) does not further improve the PDP.

4) Performance of RIPs for Mono-T Links: As noted in Remark 2, the proposed scheme can also be used to design near-optimal RIPs for mono-T EH links by simply dropping the EUR constraint at the receiver. The results in Fig. 7 compare the performance of the RIPs designed for an ARQ-based mono-T EH link with the SoC-dependent policies designed using the Markov decision process (MDP) based framework. The performance is compared for both slow and fast fading channels with different number of quantization levels for the channel gain. In theory, SoC-dependent policies designed using the MDP framework perform at least as well as, and possibly better, than the proposed SoC independent RIPs. However, in practice, the MDP is formulated by quantizing the battery and channel states, and increasing the number of quantization levels increases the computational complexity of MDP. Thus, due to the effect of quantization of the battery and channel states, in practice we find that the designed RIPs can even outperform the policies obtained using MDPs.

The results in this section illustrate that the RIPs obtained using the proposed GP based design procedure improves the PDP of the system compared to the state-of-the-art schemes. Moreover, the values of the system parameters used for the experiments correspond to practical scenarios. For example, in Fig. 5, for an ARQ-based fast fading link, the size of the battery used at the transmitter is 4000 units, which is much less than the size of the battery used in practical EHNs (see footnote 2). The results thus reaffirm that the proposed scheme is suitable for implementation in present-day EHNs.

IX. Conclusions

In this work, we designed near-optimal, SoC-unaware, retransmission index based power control policies for *dual* EH links with both slow and fast fading channels. We showed that, in the energy unconstrained regime, the performance of the proposed SoC independent policies converge asymptotically to that of the optimal policy under infinite batteries, as the size of the battery size gets large. These results characterized the battery size required to achieve a PDP sufficiently close to that of a system with infinite capacity batteries. By reformulating the problem as a geometric program, we obtained near-optimal RIPs in a computationally efficient manner. Using Monte Carlo simulations, we showed that the designed RIPs outperform state-of-the-art policies in terms of their PDP. Further extensions of this work could include the design of power control policies that account for and exploit the temporal correlation in the channel.

Appendix

A. Proof of Lemma 1

The PDP can be written as

$$P_{\mathrm{D}} = \min_{\mathcal{P}} \Bigg[\sum_{(i_1,j_1)\in I_1} \pi(i_1,j_1) P_{\mathrm{D}}(K|i_1,j_1,U_n=1) + \sum_{(i_2,j_2)\in I_2} \pi(i_2,j_2) P_{\mathrm{D}}(K|i_2,j_2,U_n=1) \Bigg], \quad (16)$$

Now, for all $(i,j) \in I_2$, $P_{\mathrm{D}}(K|i,j,U_n=1) = c$, where $c \in [0,1]$ is some constant. Recall that, in I_2, the EHNs can make all K attempts regardless of number of slots (m_t and m_r) in which the transmitter and receiver harvest the energy. Also, in I_1, the packet cannot be guaranteed to be attempted all K times, and $I_1 \cup I_2 = I$. Without loss of generality, $\forall\ (i_1,j_1) \in I_1$, we can write $P_{\mathrm{D}}(K|i_1,j_1,U_n=1) = c + \epsilon(i_1,j_1)$, where

$\epsilon(i_1, j_1) \triangleq P_{\mathrm{D}}(K|i_1, j_1, U_n = 1) - c \in [0, 1]$. Hence, for $(i, j) \in I_2$, (16) can be written as

$$P_{\mathrm{D}} = \min_{\mathcal{P}}\Big[P_{\mathrm{D}}(K|i, j, U_n = 1) + \sum_{(i_1,j_1)\in I_1} \pi(i_1, j_1)\epsilon(i_1, j_1)\Big],$$
$$\leq P_{\mathrm{D}}(K|i, j, U_n = 1)\Big|_{\mathcal{P}^*} + \sum_{(i_1,j_1)\in I_1} \pi(i_1, j_1)\Big|_{\mathcal{P}^*}, \quad (17)$$

where $\mathcal{P}^* = \arg\min_{\mathcal{P}} P_{\mathrm{D}}(K|i, j, U_n = 1)$ for any $(i, j) \in I_2$. This establishes the upper bound.

Using (16), and the fact that $\epsilon(i_1, j_1) \geq 0$ for all $(i_1, j_1) \in I_1$, $P_{\mathrm{D}}(K|i, j, U_n = 1)\Big|_{\mathcal{P}^*} \leq \min_{\mathcal{P}}\Big[P_{\mathrm{D}}(K|i, j, U_n = 1) + \sum_{(i_1,j_1)\in I_1} \pi(i_1, j_1)\epsilon(i_1, j_1)\Big]$, for all $(i, j) \in I_2$, which establishes the lower bound.

B. Proof of Lemma 2

In this proof, we omit the superscript t on battery state sets such as I_1 and I_2, as well as on the battery state at the stopping time T_i, denoted by B_{T_i}, since the result pertains only to the transmitter of the dual EH link. To prove the result, we compute the stationary probability of the set I_1, in terms of the mean time to return to the set I_1, denoted as $\mathbb{E}(T_{I_1})$. Now, $\mathbb{E}(T_{I_1}) = \mathbb{E}(T_1) + \mathbb{E}(T_2)$, where $\mathbb{E}(T_1)$ denotes the expected time when the DTMC first hits either the set I_1 or the set I_2' once it leaves I_1, and $\mathbb{E}(T_2)$ is the mean time required to visit the set I_1 starting from the set I_2' (see Fig. 8). The proof proceeds by further decomposing $\mathbb{E}(T_2)$ in terms of other hitting times.

The battery evolution at the transmitter, given by (1), can be rewritten as follows:

$$B_{n+1}^t = \begin{cases} \left\{B_n^t + \mathbb{1}_{\{E_n^t \neq 0\}} - \mathcal{L}(B_n^t, B_n^r, U_n)\right\}^+ & \text{if } B_n^t \neq B_{\max}^t, \\ B_n^t - \mathcal{L}(B_n^t, B_n^r, U_n), & \text{otherwise,} \end{cases}$$

where $\{x\}^+ \triangleq \max\{0, x\}$. Here, $\mathbb{1}_{\{E_n^t\neq 0\}}$ and $\mathcal{L}(B_n^t, B_n^r, U_n)$ are as defined in the statement of the Lemma. For a dual EH link operating in the EUR, the process $\mathbb{1}_{\{E_n^t\neq 0\}} - \mathcal{L}(B_n^t, B_n^r, U_n)$ has a positive mean drift. From renewal theory, the stationary probability of the set I_1 is $\pi_{I_1} = 1/\mathbb{E}(T_{I_1})$, where T_{I_1} is the return time to the set I_1. Now,

$$\mathbb{E}(T_{I_1}) = \mathbb{E}(T_1|B_0 \in I_1) + \sum_{i=1}^{L_{\max}} \mathbb{E}(T_2|B_{T_1} = B_{\max}^t - i) \times \Pr\left(B_{T_1} = B_{\max}^t - i|B_0 \in I_1\right), \quad (18)$$

where T_1 denotes the first time, starting from the set I_1, when the DTMC returns to the set I_1 or hits the set I_2' (see Fig. 8) and B_{T_i} denotes the battery state at time T_i for all $i \in \mathbb{N}$, while B_0 denotes the battery state at the start. Also, T_2 denotes the time taken by the DTMC to return to the set I_1, starting from a state in the set I_2', and is given as

$$\mathbb{E}\left(T_2|B_{T_1} = B_{\max}^t - i\right) = \mathbb{E}\left(T_3|B_{T_1} = B_{\max}^t - i\right) + \Pr\left(B_{T_3} = B_{\max}^t|B_{T_1} = B_{\max}^t - i\right) \times \mathbb{E}\left(T_5|B_{T_3} = B_{\max}^t\right). \quad (19)$$

Here, T_3 denotes the first time the DTMC hits the set I_1 or $B_{\max}^t$, starting from state $B_{\max}^t - i \in I_2'$. Also,

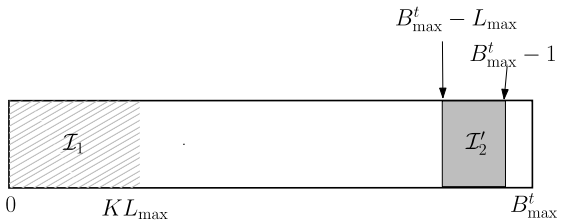

Fig. 8. Different sets of battery states used for proof of Lemma 2. Set I_1 contains the battery states $\{0, 1, \ldots, KL_{\max}\}$, while set I_2' contains the battery states $\{B_{\max}^t - L_{\max}, \ldots, B_{\max}^t - 1\}$.

T_5 denotes the time taken by the DTMC, starting from $B_{\max}^t$, to return to the set I_1. Next, $\mathbb{E}\left(T_5|B_{T_3} = B_{\max}^t\right)$ can be written in terms of T_4, which is defined as the first time the DTMC hits the set I_2' starting from $B_{\max}^t$, as follows: $\mathbb{E}(T_5|B_{T_3} = B_{\max}^t) = \mathbb{E}\left(T_4|B_{T_3} = B_{\max}^t\right) + \sum_{j=1}^{L_{\max}} \Pr\left(B_{T_4} = B_{\max}^t - j|B_{T_3} = B_{\max}^t\right) \mathbb{E}(T_2|B_{T_4} = B_{\max}^t - j)$. Since $\sum_{j=1}^{L_{\max}} \Pr\left(B_{T_4} = B_{\max}^t - j|B_{T_3} = B_{\max}^t\right) = 1$, this can be bounded as

$$\mathbb{E}(T_5|B_{T_3} = B_{\max}^t) \leq \mathbb{E}\left(T_4|B_{T_3} = B_{\max}^t\right) + \max_{1\leq j\leq L_{\max}} \mathbb{E}(T_2|B_{T_4} = B_{\max}^t - j). \quad (20)$$

Substituting the above upper bound on $\mathbb{E}(T_5|B_{T_3} = B_{\max}^t)$ in (19), maximizing both sides over all i and simplifying, we get

$$\max_{1\leq i\leq L_{\max}} \mathbb{E}\left(T_2|B_{T_1} = B_{\max}^t - i\right) \leq \mathbb{E}\left(T_4|B_{T_3} = B_{\max}^t\right) \times \frac{\max_{1\leq i\leq L_{\max}} \Pr\left(B_{T_3} = B_{\max}^t|B_{T_1} = B_{\max}^t - i\right)}{\min_{1\leq i\leq L_{\max}} \Pr\left(B_{T_3} \in I_1|B_{T_1} = B_{\max}^t - i\right)} + \frac{\max_{1\leq i\leq L_{\max}} \mathbb{E}\left(T_3|B_{T_1} = B_{\max}^t - i\right)}{\min_{1\leq i\leq L_{\max}} \Pr\left(B_{T_3} \in I_1|B_{T_1} = B_{\max}^t - i\right)}. \quad (21)$$

The denominator in the above uses the fact that hitting $B_{\max}^t$ and hitting a state in the set I_1 starting from state $B_{\max}^t - i \in I_2'$ are complementary events. Similar to (20), we can obtain a lower bound on $\mathbb{E}(T_5|B_{T_3} = B_{\max}^t)$ by considering the minimum of $\mathbb{E}(T_2|B_{T_4} = B_{\max}^t - j)$ over $1 \leq j \leq L_{\max}$. Substituting the resulting inequality in (19) and minimizing over i, we get

$$\min_{1\leq i\leq L_{\max}} \mathbb{E}\left(T_2|B_{T_1} = B_{\max}^t - i\right) \geq \mathbb{E}\left(T_4|B_{T_3} = B_{\max}^t\right) \times \frac{\min_{1\leq i\leq L_{\max}} \Pr\left(B_{T_3} = B_{\max}^t|B_{T_1} = B_{\max}^t - i\right)}{\max_{1\leq i\leq L_{\max}} \Pr\left(B_{T_3} \in I_1|B_{T_1} = B_{\max}^t - i\right)} + \frac{\min_{1\leq i\leq L_{\max}} \mathbb{E}\left(T_3|B_{T_1} = B_{\max}^t - i\right)}{\max_{1\leq i\leq L_{\max}} \Pr\left(B_{T_3} \in I_1|B_{T_1} = B_{\max}^t - i\right)}. \quad (22)$$

To compute the hitting times and probabilities in (18), (21) and (22), we need the following Lemma.

Lemma 3: The probability that, starting from a state in the set I_2', the DTMC hits the set I_1 before hitting $B_{\max}^t$ at the stopping time T_3 decays exponentially with $B_{\max}^t$. That is,

$Pr\left(B_{T_3} \in I_1 | B_{T_1} = B^t_{\max} - i\right) = \Theta(e^{r^t_* B^t_{\max}})$, where r^t_* is as defined in Lemma 2.

Proof: See Appendix C. ∎

Now, using Lemma 3 and following a procedure similar to its proof in Appendix C, we get the following results (we omit the details to avoid repetition):

$$\begin{aligned}
\Pr\left(B_{T_3} \in I_1 | B_{T_1} = B^t_{\max} - i\right) &= \Theta(e^{r^t_* B^t_{\max}}),\\
\Pr\left(B_{T_1} = B^t_{\max} - i | B_0 \in I_1\right) &= \Theta(1),\\
\Pr\left(B_{T_3} = B^t_{\max} | B_{T_1} = B^t_{\max} - i\right) &= \Theta(1),\\
\Pr\left(B_{T_4} = B^t_{\max} - j | B_{T_3} = B^t_{\max}\right) &= \Theta(1),\\
\mathbb{E}(T_1 | B_0 \in I_1) &= \Theta(B^t_{\max}),\\
\mathbb{E}(T_3 | B_{T_1} = B^t_{\max} - i) &= \Theta(1),\\
\mathbb{E}(T_4 | B_{T_3} = B^t_{\max}) &= \Theta(1),
\end{aligned} \tag{23}$$

Substituting (23) in (22), (21) and (18), we obtain $\mathbb{E}(T_{I_1}) = \Theta(e^{-r^t_* B^t_{\max}})$, where r^t_* is a negative root of the asymptotic log MGF of the drift process X^t_n. Hence, $\pi_{I_1} = \Theta(e^{r^t_* B^t_{\max}})$. To close out the proof, we need to establish Lemma 3, which is presented in the following subsection.

C. Computing the Hitting Times and Hitting Probabilities

Proof: For convenience, let $n = 0$ denote the time at which the DTMC first exits the set $I_2^{'}$. Also, let $X^t_n \triangleq \mathbb{1}_{\{E^t_n \neq 0\}} - \mathcal{L}(B^t_n, B^r_n, U_n)$. Note that, evolution of X^t_n depends on the DTMC with its state denoted by (B^t_n, B^r_n, U_n). In the following analysis, to simplify the notation, we do not explicitly show the dependence of X^t_n on the battery state at the receiver B^r_n and the retransmission index U_n. We are interested in analyzing the probability that, at the stopping time T_3, battery at the transmitter is in a state in the set I^t_1, i.e., $B_{T_3} < KL_{\max}$. To this end, we use Wald's identity for Markov modulated random walks [38, Ch. 9], written for our problem as follows

$$\mathbb{E}\left[\frac{\exp\left(r\sum_{n=1}^{T_3} X^t_n\right)}{\xi(r)^{T_3}} \frac{\pi_r(B_{T_3})}{\pi_r(B_0)}\right] = 1, \tag{24}$$

where $\xi(r)$ denotes the spectral radius of the matrix $A(r)$ whose $(i,j)^{\text{th}}$ entry is $a_{ij}(r) = p_{ij} g_i(r)$ with p_{ij} being the transition probability of the battery from state i to state j (strictly speaking, $((i_1, j_1, u_1)$ to $(i_2, j_2, u_2))$, while $g_i(r)$ denotes the generating function of the conditional distribution of X^t_n, given that $B^t_n = i$, for some $i \in I_2^{'}$, and r is any point on the real line for which $g_i(r)$ exists. In (24), π_r denotes the right eigenvector corresponding to $\xi(r)$, and $\pi_r(B)$ denotes its B^{th} element. B^{th}, which, strictly speaking, is a tuple (B^t, B^r, U_n). However, with abuse of notation, we only show its dependence on the transmitter's battery. Also, the expectation is over X^t_n. Since the process X^t_n has positive drift, there exists an $r^t_* < 0$ such that $\xi(-r^t_*) = 1$ [39]. Let q denote the probability of hitting I_1 before hitting $B^t_{\max}$. Using (24) with $r^t_{*'} = -r^t_*$, we get

$$\begin{aligned}
(1-q)\mathbb{E}\left[\exp\left(r^t_* \sum_{n=1}^{T_3} X^t_n\right) \frac{\pi_{r^t_{*'}}(B_{T_3})}{\pi_{r^t_{*'}}(B_0)} \middle| B_{T_3} = B^t_{\max}\right]\\
+ q\mathbb{E}\left[\exp\left(r^t_* \sum_{n=1}^{T_3} X^t_n\right) \frac{\pi_{r^t_{*'}}(B_{T_3})}{\pi_{r^t_{*'}}(B_0)} \middle| B_{T_3} \in I_1\right] = 1.
\end{aligned}$$

Since, for a large battery, the overshoots are negligible [38], the above can be simplified as

$$\begin{aligned}
\mathbb{E}\left[\frac{\pi_{r^t_{*'}}(B_{T_3})}{\pi_{r^t_{*'}}(B_0)}\right]\left(q\exp\left(-r^t_* B^t_{\max}\right)\right.\\
\left. + (1-q)\exp\left(r^t_* L_{\max}\right)\right) = 1.
\end{aligned} \tag{25}$$

Further, replacing the two expectation terms with their upper bounds, we get

$$q\exp\left(-r^t_* B^t_{\max}\right) + (1-q)\exp\left(r^t_* L_{\max}\right) \geq C_1', \tag{26}$$

where $C_1' \triangleq \frac{\min_{B_0} \pi_{r^t_{*'}}(B_0)}{\max_{B_{T_3}} \pi_{r^t_{*'}}(B_{T_3})}$. Thus, $q \geq C_1'' \exp\left(r^t_* B^t_{\max}\right)$. By similarly lower bounding the expectation terms in (25), it can shown that $q \leq C_2'' \exp\left(r^t_* B^t_{\max}\right)$. Hence, $q = \Theta(\exp\left(r^t_* B^t_{\max}\right))$. This completes the proof. ∎

D. Proof of Theorem 1

Proof: In this section, we denote the stationary distribution of dual EH link by $\boldsymbol{\pi_d}$, to distinguish it from the stationary distribution of mono EH links. To derive the result for the stationary distribution of a dual EH link, $\boldsymbol{\pi_d}$, we need to compute the probability of the set I_1. From Lemma 2, $\sum_{i \in I^t_1} \pi_t(i) = \Theta(e^{r^t_* B^t_{\max}})$, where $I^t_1 = I^t \backslash I^t_2$. Here, I^t is the set of all the battery states at the transmitter, and can be written as $I^t = I^t_1 \cup I^t_2$, where I^t_2 denotes the set of battery states in which all K attempts can be supported by the transmitter, irrespective of the number of slots, m_t, in which energy is harvested. Similarly, at the receiver, $\sum_{j \in I^r_1} \pi_r(j) = \Theta(e^{r^r_* B^r_{\max}})$, where $I^r = I^r_1 \cup I^r_2$, and $I^r_1 = I^r \backslash I^r_2$. The stationary distribution π_r and the sets I^r_1, I^r_2 and I_r are defined in a similar fashion as for transmitter.

Now, the stationary probability of the sets I^t_1 and I^r_1 can be written as

$$\sum_{i \in I^t_1} \pi_t(i) = \sum_{i \in I^t_1, j \in I^r_1} \pi_d(i,j) + \sum_{i \in I^t_1, j \in I^r_2} \pi_d(i,j), \tag{27}$$

$$\sum_{j \in I^r_1} \pi_r(j) = \sum_{i \in I^t_1, j \in I^r_1} \pi_d(i,j) + \sum_{i \in I^t_2, j \in I^r_1} \pi_d(i,j). \tag{28}$$

Thus, the stationary probability of the set I_1 is given as

$$\begin{aligned}
\pi_d\left((i,j) \in I_1\right) = \pi_d\left(i \in I^t_1, j \in I^r_1\right) + \pi_d\left(i \in I^t_2, j \in I^r_1\right)\\
+ \pi_d\left(i \in I^t_1, j \in I^r_2\right),
\end{aligned}$$

Adding (27) and (28) and using Lemma 2, we get

$$\begin{aligned}
2\pi_d\left(i \in I^t_1, j \in I^r_1\right) + \pi_d\left(i \in I^t_2, j \in I^r_1\right)\\
+ \pi_d\left(i \in I^t_1, j \in I^r_2\right) = \Theta(e^{r^t_* B^t_{\max}}) + \Theta(e^{r^r_* B^r_{\max}}).
\end{aligned} \tag{29}$$

The proof completes by observing that each term in the L.H.S. in (29) is nonnegative. Hence, one can upper and lower bound the L.H.S. in (29) in terms of $\pi_d\left((i,j) \in I_1\right)$. ∎

E. Dual EH Links With ARQ/HARQ-CC and Slow Fading

For a dual EH link with ARQ and slow fading channels, using [16, Lemma 3] and EUR conditions, the subproblem corresponding to $\chi = K'$ is written as

$$\min_{\tilde{\mathbf{L}}=\{L_1,\ldots,L_{K'}\}} \quad 1 - e^{-\left(\frac{\gamma_0 \aleph_0 T_p}{L_{K'} E_s \sigma_c^2}\right)}, \tag{30a}$$

$$\text{subject to} \quad \sum_{\ell=1}^{K'} L_\ell \left(1 - e^{-\left(\frac{\gamma_0 \aleph_0 T_p}{L_{\ell-1} E_s \sigma_c^2}\right)}\right) \leq K\rho_t, \tag{30b}$$

$$\sum_{\ell=1}^{K'} \left(1 - e^{-\left(\frac{\gamma_0 \aleph_0 T_p}{L_{\ell-1} E_s \sigma_c^2}\right)}\right) \leq \frac{K\rho_r}{R}, \tag{30c}$$

and $0 \leq L_1 \leq L_2 \leq \ldots \leq L_{K'} \leq L_{\max}$. The objective function above is written using the fact that, for slow fading channels with ARQ, the optimal policy is a strictly non-decreasing policy [16, Lemma 3]. The constraints in (30b) and (30c) ensure that both the transmitter and receiver operate in the EUR. Similar to the previous case, using the Taylor series expansion of e^{-x} and $Z_\ell \triangleq \frac{s}{L_\ell}$, and approximating the infinite series summations by summations of finite order, (30) can be converted to CGP, which can be solved using Algorithm 1.

For HARQ-CC, using [16, eq. 18] and EUR conditions, the subproblem corresponding to $\chi = K'$ is written as

$$\min_{\tilde{\mathbf{L}}=\{L_1,\ldots,L_{K'}\}} \quad 1 - e^{-\frac{s}{\sum_{\ell=1}^{K'} L_\ell}}, \tag{31a}$$

$$\text{subject to} \quad \sum_{\ell=1}^{K'} L_\ell \left(1 - e^{-\frac{s}{\sum_{i=1}^{\ell-1} L_i}}\right) \leq K\rho_t, \tag{31b}$$

$$\sum_{\ell=1}^{K'} \chi^\ell \left(1 - e^{-\frac{s}{\sum_{i=1}^{\ell-1} L_i}}\right) \leq \frac{K\rho_r}{R}, \tag{31c}$$

and $0 \leq L_i \leq L_{\max}$, $1 \leq i \leq K'$. The constraints in (31b) and (31c) ensure that the dual EH link operates in the EUR. Similar to the previous cases, we solve (31) using Algorithm 1. To use Algorithm 1, (31) is converted into a CGP using the Taylor series expansion of e^{-x} and defining $Z_{K'} \triangleq \frac{s}{\sum_{i=1}^{K'} L_i}$. Next, we present a method to find the optimal policies for a dual EH link with HARQ-CC and fast fading channels.

F. Dual EH Links With HARQ-CC and Fast Fading

The optimization problem for finding near-optimal RIPs for dual EH links with HARQ-CC and fast fading channels can be written in a similar manner as in previous cases, with $p_{\mathrm{o},\ell-1}$ replaced with $p_{\mathrm{out},1\to\ell-1}$. The $p_{\mathrm{out},1\to\ell-1}$ is the same as $p_D(i, j, m_t, m_r)$ and is given by [16, eq. 20], with $\Psi_1 = \ell - 1$. Specifically, the optimization problem is written as

$$\min_{\tilde{\mathbf{L}}=\{L_1,\ldots,L_K\}} \quad 1 - F_K \tag{32a}$$

$$\text{subject to} \quad \sum_{\ell=1}^{K} L_\ell (1 - F_{\ell-1}) \leq K\rho_t, \tag{32b}$$

$$\sum_{\ell=1}^{K} \chi^\ell \, (1 - F_{\ell-1}) \leq \frac{K\rho_r}{R}, \tag{32c}$$

and $0 \leq L_i \leq L_{\max}$, $\chi^i \in \{0, 1\}$, $1 \leq i \leq K$, where $F_{\ell-1} \triangleq \sum_{i=1}^{M_{\ell-1}} \sum_{j=1}^{\tau_{i,\ell-1}} \sum_{k=0}^{j-1} \frac{\chi_{i,j}(\mathbf{L}_{\ell-1})}{k!} \left(\frac{X}{L_{\{i\}}}\right)^k e^{-\frac{X}{L_{\{i\}}}}$ with $X \triangleq \frac{\gamma_0 \aleph_0 T_p}{E_s}$, $\mathbf{L}_K \triangleq \mathrm{diag}(\frac{L_1}{\sigma_c^2}, \frac{L_2}{\sigma_c^2}, \ldots, \frac{L_K}{\sigma_c^2})$, and $L_{\{1\}}, L_{\{2\}}, \cdots, L_{\{M_K\}}$ denote the distinct nonzero elements of $\mathbf{L}_K$. $\tau_{i,\ell-1}$ denotes the multiplicity of $L_{\{i\}}$, and $\chi_{i,j}(\mathbf{L}_K)$ denotes the (i, j)th characteristic coefficient of $\mathbf{L}_K$ defined in [16, eq. 21]. Note that, to find a solution for a given $\{\chi^\ell\}_{\ell=1}^K$, we need to solve $2^\chi - \chi$ subproblems, where $\chi = \sum_{\ell=1}^L \chi_\ell$. Hence, to solve (32), since χ can take values $1, 2, \ldots, K$, we need to solve $(2^{K+2} - K(K+1) - 4)/2$ subproblems, and pick the solution corresponding to the subproblem which yields the minimum PDP among them, which is computationally expensive.

Alternatively, using a result from [19, Th. 1], we can approximate the $p_{\mathrm{out},1\to\ell}$ as $p_{\mathrm{out},1\to\ell} \approx \frac{X^\ell}{\ell! L_1 L_2 \cdots L_\ell}$. Using this approximation, for a given $\{\chi^\ell\}_{\ell=1}^K$, the optimization problem in (32) reduces to a GP. Thus to solve (32), we need to solve K GPs and pick the best solution.

G. Proof of Theorem 1 for Markov Energy Harvesting Models

In this section, we present the proof of Theorem 1 when the EH process at the transmitter and receiver are temporally correlated. Note that, for the Markov model, the result in Theorem 1 is valid, provided Lemma 2 holds true in this scenario also. Thus, in the following, we discuss the proof of Lemma 2 for the Markov model.

In the Markov case, the drift process, defined in Lemma 2, modifies as $X_n^t \triangleq e_n^t - \mathcal{L}(B_n^t, B_n^r, U_n)$, where e_n^t denotes the amount of energy harvested in the n^{th} slot. For a dual EH link operating in the EUR, the process $e_n^t - \mathcal{L}(B_n^t, B_n^r, U_n)$ has a positive mean drift. From renewal theory, the stationary probability of the set I_1^t is $\pi_{I_1^t} = 1/\mathbb{E}(T_{I_1^t})$. Next, since the battery at the node still evolves in a Markovian fashion in this scenario, $\mathbb{E}(T_{I_1^t})$ is given by (18). Further, to compute (18), we use the expressions given in (19), (20), (21) and (22), which are in turn computed using the results in Lemma 3. The proof completes by noting that the result in Lemma 3 is also applicable to this scenario. This is because, X_n^t is a Markov modulated random walk, with its underlying Markov chain being the one described in the beginning of Section VII. ■

REFERENCES

[1] M. L. Ku, W. Li, Y. Chen, and K. J. R. Liu, "Advances in energy harvesting communications: Past, present, and future challenges," *IEEE Commun. Surveys Tuts.*, vol. 18, no. 2, pp. 1384–1412, 2nd Quart., 2016.

[2] X. Lu, P. Wang, D. Niyato, D. I. Kim, and Z. Han, "Wireless networks with RF energy harvesting: A contemporary survey," *IEEE Commun. Surveys Tuts.*, vol. 17, no. 2, pp. 757–789, 2nd Quart., 2015.

[3] P.-V. Mekikis, A. S. Lalos, A. Antonopoulos, L. Alonso, and C. Verikoukis, "Wireless energy harvesting in two-way network coded cooperative communications: A stochastic approach for large scale networks," *IEEE Commun. Lett.*, vol. 18, no. 6, pp. 1011–1014, Jun. 2014.

[4] A. Arafa and S. Ulukus, "Single-user and multiple access channels with energy harvesting transmitters and receivers," in *Proc. IEEE GlobalSIP*, Dec. 2014, pp. 213–217.

[5] P.-V. Mekikis, A. Antonopoulos, E. Kartsakli, A. S. Lalos, L. Alonso, and C. Verikoukis, "Information exchange in randomly deployed dense WSNs with wireless energy harvesting capabilities," *IEEE Trans. Wireless Commun.*, vol. 15, no. 4, pp. 3008–3018, Apr. 2016.

[6] S. Ulukus *et al.*, "Energy harvesting wireless communications: A review of recent advances," *IEEE J. Sel. Areas Commun.*, vol. 33, no. 3, pp. 360–381, Mar. 2015.
[7] V. Sharma, U. Mukherji, V. Joseph, and S. Gupta, "Optimal energy management policies for energy harvesting sensor nodes," *IEEE Trans. Wireless Commun.*, vol. 9, no. 4, pp. 1326–1336, Apr. 2010.
[8] M. Gregori and M. Payaro, "Energy-efficient transmission for wireless energy harvesting nodes," *IEEE Trans. Wireless Commun.*, vol. 12, no. 3, pp. 1244–1254, Mar. 2013.
[9] C. K. Ho and R. Zhang, "Optimal energy allocation for wireless communication with energy harvesting constraints," *IEEE Trans. Signal Process.*, vol. 60, no. 9, pp. 4808–4818, Sep. 2012.
[10] S. Kim, R. Fonseca, and D. Culler, "Reliable transfer on wireless sensor networks," in *Proc. 1st Annu. IEEE Commun. Soc. Conf. Sensor Adhoc Commun. Netw. (SECON)*, Oct. 2004, pp. 449–459.
[11] S. Zhou, T. Chen, W. Chen, and Z. Niu, "Outage minimization for a fading wireless link with energy harvesting transmitter and receiver," *IEEE J. Sel. Areas Commun.*, vol. 33, no. 3, pp. 496–511, Mar. 2015.
[12] A. Yadav, M. Goonewardena, W. Ajib, and H. Elbiaze, "Novel retransmission scheme for energy harvesting transmitter and receiver," in *Proc. IEEE ICC*, Jun. 2015, pp. 3198–3203.
[13] B. Medepally, N. B. Mehta, and C. R. Murthy, "Implications of energy profile and storage on energy harvesting sensor link performance," in *Proc. IEEE GLOBECOM*, Dec. 2009, pp. 1–6.
[14] A. Aprem, C. R. Murthy, and N. B. Mehta, "Transmit power control policies for energy harvesting sensors with retransmissions," *IEEE J. Sel. Topics Signal Process.*, vol. 7, no. 5, pp. 895–906, Oct. 2013.
[15] A. M. Devraj, M. K. Sharma, and C. R. Murthy, "Power allocation in energy harvesting sensors with ARQ: A convex optimization approach," in *Proc. IEEE GlobalSIP*, Dec. 2014, pp. 208–212.
[16] M. K. Sharma and C. R. Murthy, "Packet drop probability analysis of dual energy harvesting links with retransmissions," *IEEE J. Sel. Areas Commun.*, vol. 34, no. 12, pp. 3646–3660, Dec. 2016.
[17] M. K. Sharma and C. R. Murthy, "Packet drop probability analysis of ARQ and HARQ-CC with energy harvesting transmitters and receivers," in *Proc. IEEE GlobalSIP*, Dec. 2014, pp. 148–152.
[18] *IEEE Standard for Local and Metropolitan Area Networks—Part 15.4: Low-Rate Wireless Personal Area Networks (LR-WPANs)*, IEEE Standard 802.15.4-2011 (Revision. IEEE Standard 802.15.4-2006), Sep. 2011, pp. 1–314.
[19] T. V. K. Chaitanya and E. G. Larsson, "Optimal power allocation for hybrid ARQ with chase combining in i.i.d. Rayleigh fading channels," *IEEE Trans. Commun.*, vol. 61, no. 5, pp. 1835–1846, May 2013.
[20] R. D. Yates and H. Mahdavi-Doost, "Energy harvesting receivers: Packet sampling and decoding policies," *IEEE J. Sel. Areas Commun.*, vol. 33, no. 3, pp. 558–570, Mar. 2015.
[21] I. S. Kim, "Nonlinear state of charge estimator for hybrid electric vehicle battery," *IEEE Trans. Power Electron.*, vol. 23, no. 4, pp. 2027–2034, Jul. 2008.
[22] R. Xiong, H. He, F. Sun, and K. Zhao, "Evaluation on state of charge estimation of batteries with adaptive extended Kalman filter by experiment approach," *IEEE Trans. Veh. Technol.*, vol. 62, no. 1, pp. 108–117, Jan. 2013.
[23] N. Michelusi, L. Badia, R. Carli, K. Stamatiou, and M. Zorzi, "Correlated energy generation and imperfect state-of-charge knowledge in energy harvesting devices," in *Proc. 8th IWCMC*, Aug. 2012, pp. 401–406.
[24] D. Del Testa and M. Zorzi, "Optimal policies for two-user energy harvesting device networks with imperfect state-of-charge knowledge," in *Proc. IEEE Inf. Theory Appl. Workshop*, Feb. 2014, pp. 1–5.
[25] R. Srivastava and C. E. Koksal, "Basic performance limits and tradeoffs in energy-harvesting sensor nodes with finite data and energy storage," *IEEE/ACM Trans. Netw.*, vol. 21, no. 4, pp. 1049–1062, Aug. 2013.
[26] W. Su, S. Lee, D. A. Pados, and J. D. Matyjas, "Optimal power assignment for minimizing the average total transmission power in hybrid-ARQ Rayleigh fading links," *IEEE Trans. Commun.*, vol. 59, no. 7, pp. 1867–1877, Jul. 2011.
[27] J. A. Paradiso and M. Feldmeier, "A compact, wireless, self-powered pushbutton controller," in *Proc. Int. Conf. Uniquitous Comput.*, 2001, pp. 299–304.
[28] C. K. Ho, P. D. Khoa, and P. Ming, "Markovian models for harvested energy in wireless communications," in *Proc. IEEE ICCS*, Nov. 2010, pp. 311–315.
[29] K. Tutuncuoglu and A. Yener, "Communicating with energy harvesting transmitters and receivers," in *Proc. IEEE Inf. Theory Appl. Workshop*, Feb. 2012, pp. 240–245.
[30] S. Reddy and C. R. Murthy, "Dual-stage power management algorithms for energy harvesting sensors," *IEEE Trans. Wireless Commun.*, vol. 11, no. 4, pp. 1434–1445, Apr. 2012.
[31] L. Chen *et al.*, "Range extension of passive wake-up radio systems through energy harvesting," in *Proc. IEEE ICC*, Jun. 2013, pp. 1549–1554.
[32] S. Sudevalayam and P. Kulkarni, "Energy harvesting sensor nodes: Survey and implications," *IEEE Commun. Surveys Tuts.*, vol. 13, no. 3, pp. 443–461, 3rd Quart., 2011.
[33] M. Hasan and E. Hossain, "Distributed resource allocation for relay-aided device-to-device communication: A message passing approach," *IEEE Trans. Wireless Commun.*, vol. 13, no. 11, pp. 6326–6341, Nov. 2014.
[34] M. Chiang, C. W. Tan, D. Palomar, D. O'Neill, and D. Julian, "Power control by geometric programming," *IEEE Trans. Wireless Commun.*, vol. 6, no. 7, pp. 2640–2651, Jul. 2007.
[35] *GGPLAB: A Simple MATLAB Toolbox for Geometric Programming*, accessed on Feb. 2015. [Online]. Available: http://www.stanford.edu/~boyd/ggplab/
[36] A. Goldsmith, *Wireless Communications*. Cambridge, U.K.: Cambridge Univ. Press, 2005.
[37] P. Grover, K. Woyach, and A. Sahai, "Towards a communication-theoretic understanding of system-level power consumption," *IEEE J. Sel. Areas Commun.*, vol. 29, no. 8, pp. 1744–1755, Sep. 2011.
[38] R. G. Gallager, *Stochastic Processes: Theory for Applications*. Cambridge, U.K.: Cambridge Univ. Press, 2014.
[39] D. N. C. Tse, "Variable-rate lossy compression and its effects on communication networks," Ph.D. dissertation, Dept. Elect. Eng. Comput. Sci., MIT, Cambridge, MA, USA, Sep. 1994. [Online]. Available: http://www.eecs.berkeley.edu/~dtse/pub.html

Mohit K. Sharma received the B.E. degree in electronics and communication engineering from the University of Rajasthan, Jaipur, India, in 2006, and the M.Tech. degree in signal processing from IIT Guwahati, Guwahati, India, in 2010. He is currently pursuing the Ph.D. degree in electrical communication engineering with the Indian Institute of Science, Bangalore, India. His research interests are energy harvesting and resource allocation for wireless communications.

Chandra R. Murthy (S'03–M'06–SM'11) received the B.Tech. degree in electrical engineering from IIT Madras, Chennai, in 1998, the M.S. degree in electrical and computer engineering from Purdue University in 2000, and the Ph.D. degree in electrical and computer engineering from the University of California at San Diego, San Diego, CA, USA, in 2006. From 2000 to 2002, he was an Engineer with Qualcomm Inc., where he was involved in WCDMA baseband transceiver design and 802.11b baseband receivers. From 2006 to 2007, he was a Staff Engineer with Beceem Communications Inc., on advanced receiver architectures for the 802.16e Mobile WiMAX standard. In 2007, he joined the Department of Electrical Communication Engineering, Indian Institute of Science, Bangalore, India, where he is currently an Associate Professor.

His research interests are energy harvesting communications, multiuser MIMO systems, and sparse signal recovery techniques applied to wireless communications. His paper received the Best Paper Award in the communications track in the National Conference on Communications 2014. He was an elected member of the IEEE SPCOM Technical Committee for the years 2014-16, and has been re-elected for the years 2017 to 2019. He is currently serving as the Chair of the IEEE Signal Processing Society, Bangalore Chapter, and as an Associate Editor for the IEEE TRANSACTIONS ON SIGNAL PROCESSING, the IEEE TRANSACTIONS ON COMMUNICATIONS, and the *Sadhana Academy Proceedings in Engineering Sciences*. He was an Associate Editor of the IEEE SIGNAL PROCESSING LETTERS from 2012 to 2016.